PHASE I REPORT (REVISED)

MAN-COMPUTER ROLES IN SPACE NAVIGATION AND GUIDANCE

by

Eugene Farber
The Franklin Institute Research Laboratories

and

Lloyd P. Crumley and Lou Spiegel
General Electric Company

January 18, 1967

prepared for

Electronics Research Center Cambridge
National Aeronautics and Space Administration

under contract number
NAS 12-128

THE FRANKLIN INSTITUTE RESEARCH LABORATORIES
SYSTEMS SCIENCE DIVISION

This report is a revision of the Phase I report
submitted to NASA by The Franklin Institute Re-
search Laboratories on October 17, 1966, and is
submitted in accordance with the requirements of
contract NAS 12-128.

Approved:

Carl A. Silver

Carl A. Silver
Manager
Behavioral Sciences Laboratory

TABLE OF CONTENTS

LIST OF ILLUSTRATIONS

LIST OF TABLES

Section 1
INTRODUCTION

This report is a revision and an extension of The Franklin Institute Research Laboratories' Technical Memorandum 1-179, the Phase I report under Contract NAS 12-128 between The Franklin Institute Research Laboratories and NASA Electronics Research Center. The purpose of this contract is to investigate and determine the role of man in performing guidance and navigation while utilizing navigation systems of various degrees of complexity in future manned space flights. This report deals with the following subjects:

1. *Selection of a mission.* From the selected mission constraints, the required trajectories are calculated. Then, in turn, the guidance requirement in each phase and the navigation information needed for each guidance event are determined.

2. *Determination of the required navigational observations and measurement and specification of the computations to be performed on the obtained data.* From a knowledge of required observations and measures, combined with a knowledge of the state-of-the-art in measurement techniques, a first approximation to the required performances of a human operator may be obtained. Similarly, from a knowledge of the computations to be performed, an estimate can be made of the degree to whice pretabulated data or automatic data processing may be required to supplement the capabilities of the on-board personnel. The information concerning the computations to be performed is not included in this report; work to specify these computations in detail is proceeding and will be included in the Phase II report.

3. *Analysis of the sensitivity of the orbits and trajectories to guidance errors during the phase of the mission.* From these sensitivity data the cost, and therefore, the relative importance of errors in different mission phases can be determined. This information will be of crucial importance in Phase II, since the time required for the man to perform any given function—and on occasion his ability to perform the task at all—will depend in part on the accuracy requirements.

4. *Determination and description of various types of automatic and manual navigation sensors capable of providing the required data.* This information forms the basis for synthesizing two approaches to space navigation and guidance: an aided-manual approach and a semiautomatic approach. Consideration of two basic approaches does not indicate a recommendation of either or both; the particular sets of equipment utilized in a given space mission will be specially selected, and in part specially designed, for that mission. However, the data resulting from this study should serve as a basis for estimating man-machine requirements for any given system configuration.

The overall structure of the research program is shown in a program flow chart, Figure 1-1; the numbers on this figure are keyed to the items in Table 1-1. Although this flow chart is currently being updated and, consequently, no longer represents precisely the sequence of activities in this research effort, it provides a reasonably accurate guide for the overall program. The present report includes, with minor exceptions, all the information in items 1 through 18 and parts of items 19 and 20. Item 21 also is included in considerable, but not final, detail.
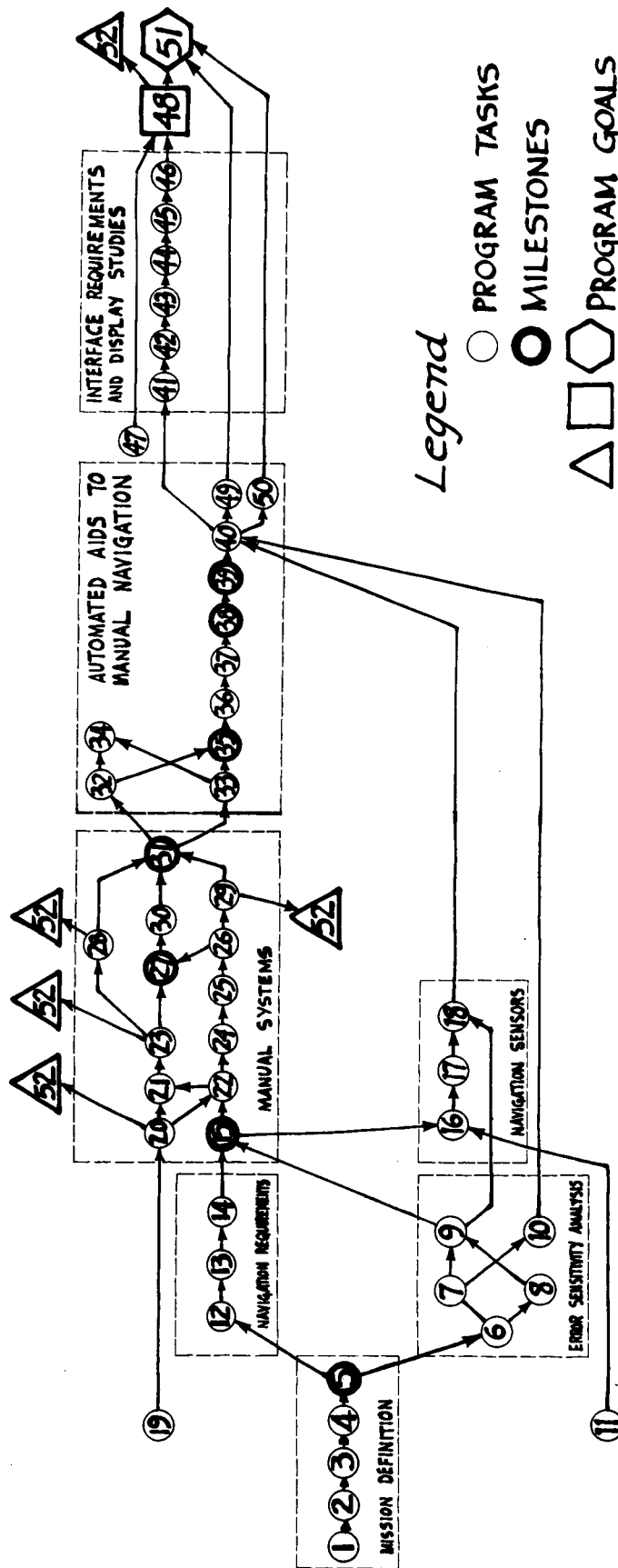
Figure 1-1. Program Flow Chart

Table 1-1. Program Events

1. Start.

2. Select mission for study.

3. Break mission down into phases.

4. Determine N & G events in each phase.

5. Specify orbits and/or reference trajectories for each phase.

6. For each phase estimate terminal velocity error as a function of initial velocity errors (pointing and burn time).

7. For each phase estimate terminal velocity error as a function of position determination errors.

8. For each phase estimate terminal velocity errors as a function of present velocity determination errors.

9. For each guidance event estimate maximum acceptable present position and velocity determination errors.

10. Indicate points of maximum sensitivity to position velocity determination and pointing errors.

11. Perform review of state-of-the-art in autonomous-automated space navigation sensor systems.

12. Indicate time of occurrence of each guidance event.

13. Specify navigation information required for each guidance event.

14. Determine measurements required to obtain the navigation information.

15. Determine measurement accuracy requirements.

16. Indicate type of sensor required in each phase.

17. Determine accuracy limitations of sensors.

18. Estimate in each phase the guidance errors probable with an automatic-autonomous navigation system.

Table 1-1. Program Events (cont)

19. Perform a review of minimal manual navigation techniques.

20. Determine for each type of measurement the expected accuracy available with manual techniques.

21. For each phase indicate the instruments and procedures required to perform navigation measurements.

22. Determine the number of observations required for each measurement to obtain acceptable accuracy.

23. Define measurement procedures in detail.

24. Determine data processing requirements associated with each observation.

25. Define minimum data processing equipment requirements.

26. Determine data processing steps in detail.

27. Summarize previous steps in detailed narrative description of minimal manual navigation and guidance system.

28. Estimate time required to perform measurement tasks.

29. Estimate time required to perform data processing tasks.

30. Establish time based N & G system information flow.

31. Perform a time line task analysis of all N & G system functions.

32. Identify peak work load periods.

33. Determine peak work load values.

34. Determine minimum crew required to perform N & G functions.

35. Determine which tasks are most costly in man hours.

36. Automate those tasks which account for the work load peaks.

Table 1-1. Program Events (cont)

37. Determine new crew functions.

38. Determine man hour savings realized.

39. Estimate savings in $\triangle V$ error (if any) attributable to automation over manual system.

40. Allocate to more sophisticated devices those tasks which man performs least accurately and/or which occur at peak error sensitivity points.

41. State the man/machine task allocation.

42. Establish man/machine interface requirements on a preliminary basis.

43. Draw a functional block diagram of semi automatic N & G system.

44. Establish semi-automatic N & G system information flow on a time base.

45. Perform a time-like task analysis of semi-automatic N & G system.

46. Specify man/machine interface requirements in detail.

47. Perform a review of the state-of-the-art in space-craft displays.

48. Specify display, control and work station requirements.

49. Indicate work load savings.

50. Estimate velocity error savings.

51. Perform a phase by phase comparison of the different configurations on the basis of man hour requirements, velocity error costs and equipment costs.

52. Indicate future research requirements.

SECTION 2
MISSION DESCRIPTION

This report describes the navigation and guidance requirements of a manned, deep-space mission; these requirements will form the basis for later work to determine whether manual navigation and guidance systems are feasible for space flights beyond the moon. "Feasible" in this context means that the manual system must promise acceptable accuracy; that it must be less complex than an automatic system and, hence, more suitable for extended missions; that it must be operable within the constraints imposed by the other systems; and that it be acceptable from a crew task-load standpoint.

2-1. GENERAL MISSION CONSTRAINTS

Future design studies in this area will require that certain related information be available for possible trade-off analysis and that the navigation and guidance problem be considered in a context which permits conclusions to be drawn in terms of some particular set of constraints. Thus, it is desirable to base this study on a mission for which a nominal trajectory and tentative mission systems can be described; with such a base, the navigation and guidance system(s) under study can be evaluated against other specifically stated system factors.

It would be possible to consider a particular trajectory and to disregard the fact that no other systems, such as a life-support or communications system, were available for discussion in the same mission context. This approach, however, would preclude the opportunity to compare navigation and guidance system changes in terms of their effect on other factors.

Early in this phase of the study the Project ARES Mission (Benjamin and Hester, 1965) was suggested as a base mission; because no better

developed feasibility study was found, the ARES mission is still the base mission for this study.

2-2. *Project ARES Mission*

The Project ARES report describes a manned mission to Mars. The mission, which was developed to take advantage of the highly favorable Earth-Mars-Venus positions during the 1984 opposition, involves a six-man crew and postulates both a Mars landing and a Venus flyby. Although several flyby options are described in the ARES study, it appears most logical to consider a direct Mars transfer with a Venus flyby on the return trip as a base mission; that option makes better use of the Venus flyby as an energy conservation tool.

The schedule of events for the base mission is shown in Table 2-1; Figure 2-1 shows the interplanetary trajectory in a sun-centered reference. Some events differ from ARES events as a result of factors introduced when an *autonomous* navigation and guidance system is defined for the mission.

2-3. *Equivalence of Trajectories*

To ensure adequate mission analysis, it is assumed that a nominal trajectory is determined on earth before the flight, and that on-board navigation and guidance consists of determining and correcting for deviations which may occur as the mission progresses. The reasons for this basic approach are beyond this study; however, they generally reflect the state-of-the-art in space-vehicle design and computer technology.

Weight restrictions resulting from thrust limitations impose severe constraints on space vehicles; missions, however, tend to have requirements which work to overextend the available energy. As a result, vehicle designers must know the exact mission to trade off alternatives for the optimal vehicle design. Once designed and built, a vehicle cannot easily undertake a mission which deviates substantially from the one for which

Table 2-1. Mission Events

Event	Julian Date (244-)	Calendar Date
Earth Launch	5580	Sept. 3, 1983
Injection to Mars	5581	Sept. 4, 1983
Final Velocity Corrections and Vehicle Spinup	5601	Sept. 24, 1983
Spindown and Initial Terminal Navigation Sightings	5818	April 8, 1984
Mars Orbit Arrival	5833	May 6, 1984
Station Keeping Begins	5834	May 7, 1984
Injection to Venus	5880	Oct. 8, 1984
Final Velocity Corrections and Vehicle Spinup	5895	Oct. 23, 1984
Spindown and Initial Flyby Navigational Sightings	6059	Dec. 27, 1984
Venus Flyby	6074	Jan. 10, 1985
Final Velocity Corrections and Vehicle Spinup	6089	Jan. 25, 1985
Spindown and Initial Terminal Navigation Sightings	6190	May 6, 1985
Earth Arrival	6210	May 26, 1985

VENUS ORBIT

FLY BY 6074

EARTH ORBIT

MARS ORBIT

RETURN 6210

S

VERNAL EQUINOX

ARRIVE 5834

1984 OPPOSITION

LEAVE 5880

LAUNCH 5580
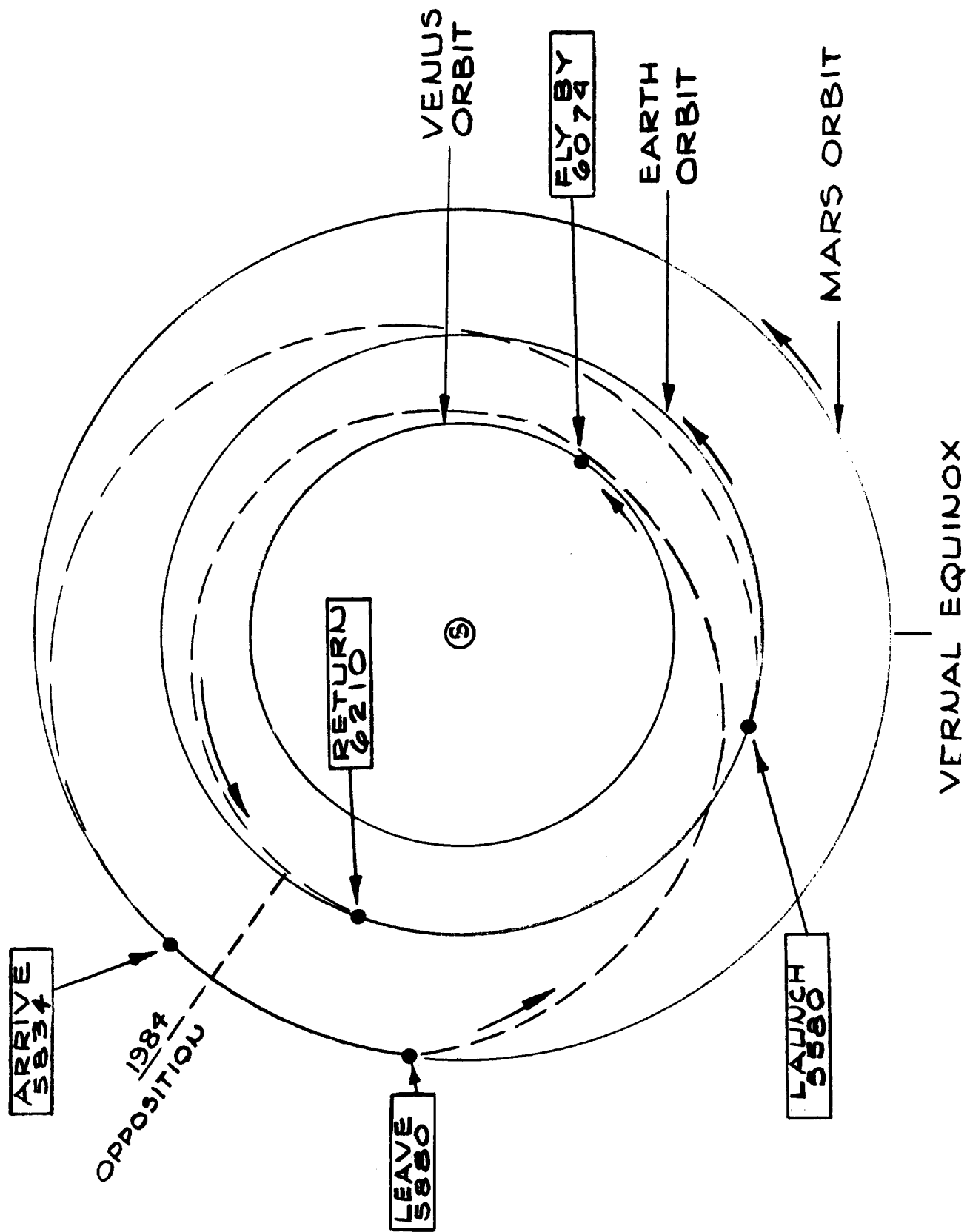
Figure 2-1. *Major Mission Events in Sun-Planet Reference*

2-4

it was designed; thus, once a vehicle is launched, the range of options available to it is limited.

In addition to weight restrictions, the problems of selecting between-trajectory classes and computing trajectories is significant. These activities require hardware, software, and skills that probably will not be available in space vehicles for some time. Therefore, most authorities consider that a "perturbation" approach to interplanetary navigation should be employed, in which course deviations are compensated for by determining the guidance required to put the vehicle onto the available course option which best approximates the nominal trajectory. The design of the ultimate hardware, and the success of the mission after launch, require that a mission use a trajectory "equivalent" to the one defined for the mission. The mission described for this study involves a major leg of 252 days which begins and ends at specific points in the solar system. Since no adequate trajectory data were found for this exact mission, the problem arose of determining what was an equivalent trajectory.

Trajectory analysts at the General Electric Re-Entry Systems Department indicated that time was the important parameter and that a trajectory with the same Earth-to-Mars time would be equivalent, even though the distance covered or the departure and arrival positions for the planets differed. They also indicated that all time-equivalent missions of a particular class had essentially similar error sensitivities, and that while minor differences between missions in a class could have important influences on total system development they would have no significant impact on the navigation and guidance system itself. It was therefore concluded that any 252-day mission of the "high-energy" class could be used and a trajectory from Clarke, *et al*. (1964) was selected. The trajectory data are shown in Table 2-2; the notation used in the table is defined in Appendix A.

2-4.   Autonomous Navigation and Guidance Requirement

Another constraint on the base mission and the navigation and

Table 2-2.

Heliocentric Data for a 252-Day Earth-Mars Trajectory

Parameter*	Value	Parameter*	Value	Parameter*	Value
RL	151.96	RP	249.20	RC	163.807
LAL	0	LAP	1.80	GL	-13.81
LOL	301.00	LOP	152.57	GP	13.86
VL	32.816	VP	19.883	ZAL	156.45
GAL	-13.23	GAP	11.55	ZAP	144.31
AZL	93.44	AZP	87.07	ETS	160.58
HCA	211.62	TAL	301.52	ZAE	167.00
SMA	198.14	TAP	153.13	ETE	81.16
ECC	0.32225	RCA	134.29	ZAC	91.83
INC	3.4366	APO	261.99	ETC	266.60
V1	29.318	V2	21.975	CLP	146.77

*Defined in Appendix A.

guidance systems is that all navigation and guidance must be performed on-board by a fully autonomous manned system. The purpose of this constraint is to ensure that maximum consideration is given to man's role in space navigation and guidance.

2-5. NAVIGATION AND GUIDANCE EVENTS

An interplanetary mission consists of a complex sequence of navigational and guidance events. However, the complexity can be reduced and conceptualization simplified if the base mission is considered as a series of lesser missions, each involving its own vehicle. The base mission will therefore be considered as three descrete cycles: an earth-centered cycle, an interplanetary cycle, and a Mars-landing cycle.

Earth-centered mission operations include the launch, rendezvous, and reentry of two ferry vehicles, one of which delivers the mission crew to the previously assembled mission vehicle and then returns the checkout crew to earth, and the other of which rendezvouses with the returning mission vehicle and returns its crew to earth. The interplanetary cycle involves all other mission phases except those mission events undertaken by the vehicle that descends and returns to the interplanetary vehicle from the Martian surface.

2-6. *Earth Cycle*

The base mission assumes that, several weeks before the injection window, the mission vehicle is launched into a suitable parking orbit. It is then checked out and made ready by a checkout crew. Shortly before the injection date, the mission crew is launched in a six-man ferry vehicle. The vehicle then maneuvers into the proper orbit and a rendezvous is performed. The mission crew then boards the mission vehicle and the checkout crew begins its return to earth in the ferry vehicle. The landing sequence involves an adjustment into an orbit from which a ballistic reentry can be performed.

After the mission is completed, a similar set of phases occur. The returning mission vehicle enters and maneuvers into a suitable orbit. A ferry vehicle is then launched and the rendezvous-and-exchange cycle is repeated.

It is assumed that ballistic reentries are used so that the control and navigation of maneuverable vehicles need not be considered. Such an assumption avoids the requirement of an extraordinary level of space-vehicle piloting by either the checkout crew on its return to earth, or by the returning mission crew — which would certainly be out of practice after nearly two years in nonpilot roles.

It is also assumed that the ferry vehicle can use ground-based tracking data without violating the fully autonomous navigation and guidance requirement. This assumption appears permissable because ephemeris data concering the assembled vehicle and the returned vehicle would be available from ground facilities; such data are equivalent to the planetary and star-position data that will be obtained on earth but taken on the mission for use as required.

2-7. *Interplanetary Cycle*

The flight crew must ensure that the assembled vehicle is in the proper orbit for injection into an Earth-Martian trajectory. If the orbit is not suitable, it must be corrected before the injection window opens. The interplanetary mission phases then proceed as described in Section 3.

2-8. *Mars Excursion Cycle*

The Mars exploration involves essentially the same mission phases as are involved in the Earth-centered ferry portions of the mission. However, the phases are in reverse order because the Mars exploration begins with a vehicle launched from the orbiting mission vehicle, and terminates when the returning exploration module rendezvouses with the primary mission vehicle. These phases, and those in the Earth-centered mission cycle, are also described in Section 3.

Section 3
NAVIGATION AND GUIDANCE PHASE DESCRIPTIONS

In this section the base mission is divided into a series of phases, each of which contains discrete navigation and guidance requirements. The 27 phases of the nominal mission are shown graphically in Figure 3-1. Each phase is described briefly; these descriptions will help reclassify the phases into a series of more basic functions which are the basis for the balance of the study.

3-1. EARTH CYCLE, PART 1

3-2. *Earth Launch*

The earth-launch phase begins when the crew enters the ferry vehicle and terminates when the vehicle is successfully injected into earth orbit.

3-3. *Earth-Orbit Correction*

Ideally, the inital earth orbit should be close enough to the mission vehicle to permit immediate initiation of the rendezvous; however, the mission navigation and guidance sequences are based on the assumption that a separate orbit adjustment before rendezvous may be required. During this phase, the ferry-vehicle crew determines the orbit into which their vehicle has been placed and their position relevant to the mission vehicle. Orbital corrections are then made and the ferry vehicle is moved into position for the rendezvous attempt.

3-4. *Rendezvous*

After the ferry vehicle is brought into the proper position, it will rendezvous with the mission vehicle. Rendezvous and the transfer of the two crews may be accomplished with or without physical mating of

Figure 3-1. Representation of Navigation and Guidance Phases in Sequence

the vehicles; in either event, the flight crew assumes control of the mission vehicle and the checkout crew returns to earth in the ferry vehicle.

3-5. INTERPLANETARY CYCLE

3-6. *Orbit Adjustment*

After the mission crew has assumed command of the mission vehicle, they will check its orbit and make any adjustments necessary to ensure that the vehicle can be injected at the optimal time and place.

3-7. *Cis-Martian Injection*

At the proper time, the vehicle is stabilized and power applied. Sufficient velocity is imparted to inject the mission vehicle into a Mars trajectory.

3-8. *Post-Earth Adjustment*

After the cis-Martian injection, the crew evaluates vehicle condition and determines the trajectory. Corrections are made, as required, during a period beginning about 2 days after injection and ending a maximum of 20 days later.

3-9. *Mars Terminal Adjustment*

Fifteen days before arrival at Mars, terminal navigational processes begin. Corrections are made as required to ensure entry into the correct Martian orbit.

3-10. *Mars-Orbit Entry*

At an appropriate time, the vehicle is positioned and a negative impulse imparted to it; the slowed vehicle then enters an orbit around Mars.

3-11. *Mars-Orbit Adjust*

After the vehicle has entered a Martian orbit, the crew determines the orbit and makes necessary corrections so that the mission vehicle is in the planned station-keeping orbit.

3-12. *Station Keeping*

After the mission vehicle has been placed in the proper station orbit, its crew performs any necessary navigation and guidance functions required to remain in this orbit. They also perform the mapping tasks required to select a landing site. After a site has been selected, the required lander trajectories are determined and the Mars lander is launched. Station keeping then continues until the lander crew is recovered and the next mission vehicle phase is required. While the lander is on Mars, the station crew continually updates launch time and trajectory data for the lander crew.

3-13. *Orbit Adjustment*

After the Mars lander crew has been recovered, the orbit is checked and corrected if necessary for optimal cis-Venutian injection.

3-14. *Cis-Venutian Injection*

This phase is similar to the cis-Martian injection previously described.

3-15. *Post-Mars Adjustment*

The post-Mars adjustment is similar to the post-Earth adjustment, except that it must be completed by the 15th day after injection; by this time, the accuracy of the navigation system would be extended to its limit because of Mars' smaller diameter.

3-16. *Venus Terminal Adjustment*

This adjustment is similar to the already described Mars terminal adjustment, except that, again, the disc size of Venus would require that a closer approach (15 days) be made before adequate sightings could be obtained.

3-17. *Venus Flyby*

The flyby phase is a special case of orbital entry. As the vehicle passes Venus, a velocity correction may be required to correct either exit velocity or the trajectory inclination. Although these corrections do not result in an orbit around Venus, they do change the direction at which the vehicle leaves the influence of Venus.

3-18. *Post-Venus Adjustment*

This phase is similar to the post-Earth and post-Martian adjustment phases, but again the differing planet size varies the time by which the final adjustment must be made in order not to make corrections based on sightings where instrument error is significant.

3-19. *Earth Terminal Adjustment*

Similar to previously described terminal adjustments, this phase begins 20 days before scheduled earth arrival.

3-20. *Earth-Orbit Entry*

Initial entry for the returning spacecraft is to a relatively high orbit which will minimize the criticality of the entry maneuvers. Options for the initial orbital entry may be available.

3-21. *Earth-Orbit Adjustment*

After an initial earth orbit has been reached, the crew determines the orbit and calculates the necessary adjustments required to put the vehicle into the terminal orbit. The final orbit will be selected from

orbits defined prior to launch so that a ferry vehicle can be ground-launched into an orbit where it can rendezvous with the returning vehicle. After the final orbital adjustment, the crew will station-keep until the ferry vehicle arrives.

3-22. EARTH CYCLE, PART 2

3-23. *Earth Ferry Rendezvous*

The ferry vehicle will arrive, be maneuvered to a rendezvous position, and a rendezvous performed. After rendezvous, the returning Mars mission crew will transfer for the return to Earth.

3-24. *Earth Landing-Orbit Correction*

After transfer of the crew and of the material being returned to earth, with them, the ferry-vehicle orbit will be checked and corrected to the optimal reentry orbit.

3-25. *Earth Landing*

After the ferry vehicle has entered the final orbit, the reentry sequence will be initiated.

3-26. MARS CYCLE

3-27. *Mars-Lander Orbit Correction*

The orbit selected as optimal for station-keeping probably will not be optimal for terminal descent of the lander. Consequently, after leaving the main vehicle, the lander crew will have to correct the orbit to position their vehicle properly for the Mars landing.

3-28. *Mars Landing*

After the landing vehicle is maneuvered into a suitable initial position, it will land and preparations will be made so that an abort can

be executed if required. An updated abort plan, and nominal return plan, must be maintained during the exploration.

3-29. Mars Launch

After the exploration period, or if an abort is required, the lander vehicle will be prepared for launch and injected into orbit.

3-30. Mars-Lander Orbit Adjustment

After the lander has been successfully injected into orbit, the orbit will be determined and corrections made to position the lander vehicle for rendezvous.

3-31. Mars-Station Rendezvous

The rendezvous phase may involve docking, or it may require only a close approach, during which time the exploration crew and their collected material may be transferred to the main vehicle. In either case, the lander is jettisoned after the transfer is completed.

3-32. CLASSIFICATION OF PHASES BY FUNCTION

Although the base mission involves 27 sequential phases, a separate navigation-and-guidance approach is not required for each phase. Many phases are repetitions of earlier phases, and others are essentially similar. In Table 3-1, the various mission phases are grouped by basic function. It is apparent from Table 3-1 that the navigation and guidance requirements for the base mission can be considered in terms of eight general functions, rather than the 27 phases described earlier.

3-33. FUNCTIONS DELETED FROM CONSIDERATION

To constrain the total study effort within the implicit bounds set by the interplanetary aspect of the base mission, it is desirable to omit some functions noted in Table 3-1 from further consideration; launch, rendezvous, and landing have, therefore, been excluded. Also, no

Table 3-1. Mission-Cycle Phases Classified by Function

Function	Phase of Mission Cycle*			No. of Phases in Functional Group
	Earth	Interplanetary	Mars	
Launch	3-2	-	3-29	2
Orbit adjustment	3-3, 3-24	3-6, 3-4, 3-13, 3-21	3-27, 3-30	8
Rendezvous	3-4, 3-23	-	3-31	3
Injection	-	3-6, 3-14	-	2
Post and terminal adjustments	-	3-8, 3-9, 3-15, 3-16, 3-18, 3-19	-	6
Orbit study	-	3-10, (3-17), 3-20	-	3
Station keeping	-	3-12	-	1
Landing	3-25	-	3-28	2
Totals	6	16	5	27

*Heading numbers under which phases are described.

"midcourse correction" is included in the general sense; that is, no navigation and guidance function is described for the portions of the trajectory when the spacecraft is midway, or approximately midway, between planets. The reasons for omitting these functions are discussed under the following headings.

3-34. *Planetary Launch*

The basic requirements for the navigation and guidance of a vehicle during launch have been simply stated by Muckler and Obermayer (1964) as, "The problem ... of arriving at a certain altitude, a specific velocity, and a desired geographic coordinate with an intact vehicle." In both the Earth-launch and Mars-launch mission phases, this definition describes the problem: the desired trajectory must be selected from a limited number of possible trajectories which can provide the altitude, velocity, and geographic coordinates required to permit rendezvous without exceeding vehicle or crew limitations. However, other, more stringent, problems overshadow the problems of navigation and guidance. The launch problem from an Earth site, and probably from a Martian site, is primarily a dynamic control problem. Launch studies have been performed in which operators flew against computer simulations of launch situations. Muckler and Obermayer (1964), for example, indicate that their subjects, flying boosters in a computer simulation, could control the trajectory (although not to required terminal constraints) as long as conditions were within the normal limits. However, events that resulted from malfunctions, and many nearly normal conditions that are faced in an ascent, apparently perturbated the vehicle enough to exceed mans' capability to react. Holleman, Armstrong, and Andrews (1960) called attention to a series of factors, such as loss of thrust, windshears, vehicle separation, and burnout, as events that caused loss of control. They also identified vehicle flexibility as a severe constraint on control effectiveness.

The extent to which these parameters exist during Earth and Martian launch differs. For example, because of its soft-landing requirements, a Mars lander must be substantially more rigid than is the typical booster,

and the Mars atmosphere will probably exhibit less of the kinds of turbulence that cause windshear. Environmental and performance factors also differ, indicating that a Mars launch will involve lower g loads, less vibration, and reduced exposure to acoustic noise — all reductions that increase mans' capability to perform. Despite these differences, however, even the Martian launch situation is basically a control problem and, as such, is also beyond the scope of this study.

3-35. *Rendezvous*

Extensive literature exists in the area of rendezvous and docking. All of it, and flight experience to date, indicate that this mission phase can be accomplished with a minimum of equipment and that, with suitable training, fuel expenditures are not excessive. In general, man appears more capable at close ranges, but he can also perform reasonably well during maneuvers from longer distances.

Levin and Ward (1959) found, for example, that with appropriate displays man performed the docking maneuver with great precision and flexibility, and that with training he could control longer approaches — but with 20 to 30 percent excessive fuel consumption. Farber, *et al.* (1963), Pennington, *et al.* (1965), and Clark (1965) generally agree that this mission phase is clearly within mans' capability, and that only a minimum of information is required for good performance. Therefore, this function apparently can be safely assigned to an operator, if required, and no great effort need be applied to further analysis of it during this study.

3-36. *Landing*

The problems of orbital entry and landing partly overlap, and the literature tends to merge terminal adjustments, orbital flight, and landing into a single phase; however, the results can be separated to some extent. Foudriat and Wingrove (1961) concluded that pilots could fly reentry sequences which were of such a nature that they involved skip trajectories, orbital insertions, or direct planetary descents. Wingrove, *et al.* (1964), who studied the Apollo-type vehicle and return trajectory,

also concluded that man could control the nominal entry and could monitor and recover from a skip-out trajectory. Moul and Schy (1965) also reported adequate performance with a blunt-nose type vehicle. Miller (1965) discusses several studies in his review of the available literature, which supports the conclusion that manual control is feasible for low-lift vehicles. It appears, however, that the more highly maneuverable vehicles have dynamic characteristics which make purely manual control undesirable and dictate provision of a relatively complex on-board computational facility and a highly sophisticated automatic system.

The studies noted above, and flight experience, indicate that earth landings with low-lift-ratio vehicles are possible with relatively simple man-operated systems. A Mars landing, or landing with a high-lift vehicle in Earth atmosphere, is more complex, although Apollo studies on LEM, experience in various high-performance aircraft (X-15), and experimental vehicle flights appear to support the conclusion that an essentially manual mode will provide adequate landing control, provided that the proper initial conditions can be established.

Therefore, for this study, it is desirable to exclude the landing phase from consideration because the base mission assumes a ballistic earth entry from orbit with a low-lift vehicle, and the Mars landing involves extensive control-dynamics problems similar to those already noted as implicitly excluded in the launch phase.

3-37. *Venus Flyby*

The Venus flyby is analyzed only in terms of its phases: a terminal adjustment, a post-planet adjustment, and a flyby adjustment (which is a special case of orbit entry).

3-38. *Midcourse Correction*

Our study indicates that a midcourse correction would not be desirable with an autonomous vehicle navigation and guidance system because the planet measures used to determine position create a residual error which

becomes more significant as the distance from the planet increases. Ulti-
mately, the planet phonomena measured create an error which becomes larger
than any trajectory error that might exist. Thus, it is not feasible to
base velocity corrections on sightings taken too far from the planets in-
volved. For Earth, the maximum distance, based on the reference trajec-
tory velocities, is reached in about 20 days; for Venus and Mars, which
are smaller, the limit is about 15 days.

Therefore, this study considers only "post-planet" and "terminal"
adjustments to the trajectory, and avoids the spindown-spinup sequence
that would be required if navigational events occurred at midcourse.
This exclusion is not serious, however, because a midcourse correction
would use the same equipment and require the same operator activities as
the post-planet and terminal adjustments.

Section 4

ERROR-SENSITIVITY ANALYSIS

It is vital to the success of any manned interplaneary flight that the spacecraft proceed on the intended trajectory, because uncorrected departure from the design trajectory will cause the spacecraft to miss the intended target. The following analysis was performed in an attempt to determine the sensitivity of the base trajectory to a selected group of possible errors and to determine the velocity impulse that would have to be applied to correct the asymptotic velocity as a function of errors in these variables.

Error-sensitivity analyses were performed on four phases: Navigation and guidance: cis-Martian injection, post and terminal adjustments, Venus flyby and Mars orbit entry. The study was limited to these four specific functions because the analysis results are applicable to the other phases.

The error variables considered in each phase are as follows:

1. Cis-Martian injection -

    Altitude,

    Injection velocity,

    Flight-path angle, and

    Position in earth orbit at time of injection.

2. Post and terminal adjustments -

    Flight-path angle.

3. Venus flyby -

    Magnitude of impact parameter.

4. Mars-orbit entry -

    Mars-orbit entry altitude

In the derivation of all sensitivity coefficients, it was assumed that, the craft is injected at perigee of the departure hyperbola, and that

all thrusting is impulsive. It was also assumed that any departure of the variables from the nominal is small (this allows linearization of any equations involving sines or cosines of angle).

4-1. INJECTION

In leaving earth from a circular parking orbit, the direction and magnitude of the velocity vector at infinity (Hyperbolic excess-velocity vector) are a function of the injection velocity, altitude of the orbit, flight-path angle, and location of injection. Any departure in these quantities from the nominal will point the departure hyperbolic asymptote in an undesired direction, and will carve an error in the hyperbolic excess-velocity magnitude. The velicity impulse required to correct the asymptotic velocity can be resolved into two components, δV_T and δV_N. Component δV_T is along the direction of the velocity vector, and δV_N is perpendicular to the velocity vector, but in the plane of the trajectory. (See Figure 4-1).

The δV_N and δV_T components can be expressed as

$$\delta V_T = \left(\frac{dV_T}{dV_i}\right)\delta V_i + \left(\frac{dV_T}{dh}\right)\delta h + \left(\frac{dV_T}{d\Gamma}\right)\delta\Gamma + \left(\frac{dV_T}{dx}\right)\delta x \qquad \text{Eq. 1}$$

$$\delta V_N = \left(\frac{dV_N}{dV_i}\right)\delta V_i + \left(\frac{dV_N}{dh}\right)\delta h + \left(\frac{dV_N}{d\Gamma}\right)\delta\Gamma + \left(\frac{dV_N}{dx}\right)\delta x \qquad \text{Eq. 2}$$

where

δV_i = error in injection-velocity magnitude,

δh = error in altitude of orbit,

$\delta\Gamma$ = flight-path angle error, and

δ_x = error in location of injection

These relationships are shown pictorially in Figure 4-1.

In deriving these partials, it is assumed that the perigee of the departure hyperbola is the injection point, so that the nominal path angle at injection is zero.

Table 4-1. *Injection-Error Partials*

Velocity-Impulse Component	Injection-Error Partial*			
	δX	δh	δV_i	$\delta \Gamma$
δV_T	0	$\dfrac{\mu}{R_i^{\,2} V_\infty}$	$\sqrt{1 + \dfrac{2\mu}{R_i V_\infty^{\,2}}}$	0
δV_N	$\dfrac{1}{1 + \dfrac{R_i V_\infty^{\,2}}{\mu}} \times \dfrac{V_\infty}{R_i}$	$\dfrac{\sqrt{1 + \dfrac{2\mu}{R_i V_\infty^{\,2}}}}{1 + \dfrac{R_i V_\infty^{\,2}}{\mu}} \times \dfrac{V_\infty}{R_i}$	$\dfrac{2}{1 + \dfrac{R_i V_\infty^{\,2}}{\mu}}$	$\dfrac{2 \times \dfrac{R_i V_\infty^{\,2}}{\mu}}{1 + \dfrac{R_i V_\infty^{\,2}}{\mu}} \times V_\infty$

* μ = gravitation constant of planet

R_i = radius of injection

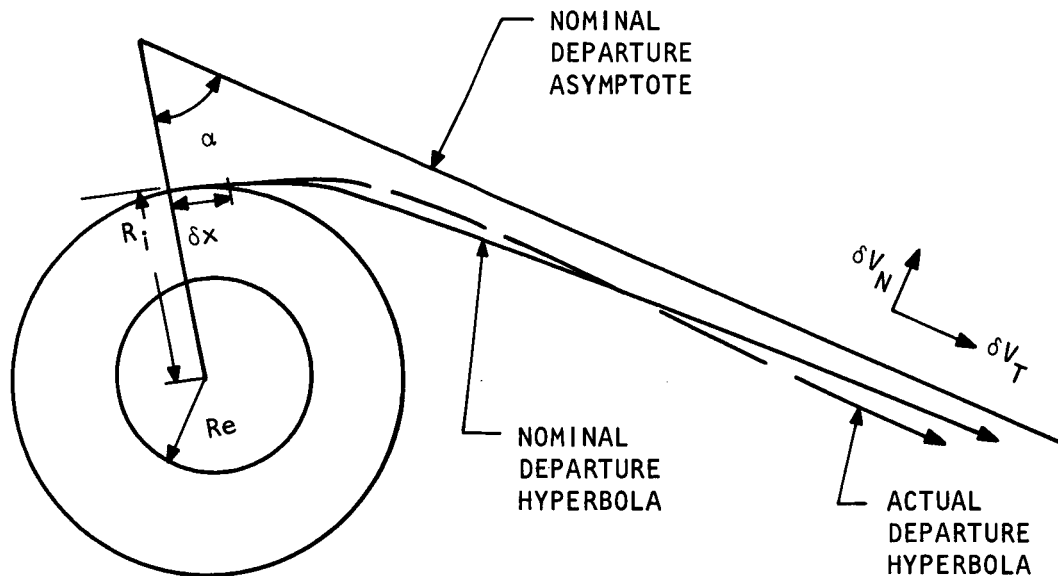V_∞ = velocity excess at infinity

Figure 4-1. *Injection Geometry*

The partials were derived as follows. The magnitude of δV_N is given by

$$\delta V_N = V_\infty \, \delta\alpha \qquad\qquad \text{Eq. 3}$$

but

$$\cos\alpha = -1/e$$

so that equation 3 may be rewritten as

$$\delta V_N = V_\infty \left(\frac{\cot\alpha}{e}\right) de. \qquad\qquad \text{Eq. 4}$$

Now δ_e may be expressed as

$$\delta_e = \frac{2R_i V_\infty}{\mu} \, \delta V_\infty \, . \qquad\qquad \text{Eq. 5}$$

And since

$$V_i^2 = V_\infty^2 + 2\,\mu/R_i \qquad\qquad \text{Eq. 6}$$

and

$$V_i \, \delta V_i = V_\infty \, \delta V_\infty, \qquad\qquad \text{Eq. 7}$$

substituting the expression for δ_e in Equation 4,

$$\delta V_N = \frac{2R_i V_\infty \cot\alpha}{e\mu} \, \delta V_i \, . \qquad\qquad \text{Eq. 8}$$

In addition,

$$\cot\alpha = \frac{\mu}{V_\infty V_i R_i} \, .$$

Therefore,

$$\delta V_N = \frac{2}{e} \, \delta V_i = \frac{2}{1 + \dfrac{R_p V_\infty^2}{\mu}} \, \delta V_i \, . \qquad\qquad \text{Eq. 9}$$

The variation of δV_N with δR_i can be similarly found.

4-4

$$\delta V_N = V_\infty \frac{\cot\alpha}{e} d_e \qquad \text{Eq. 10}$$

but

$$e = 1 + \frac{R_i V_\infty^2}{\mu} \qquad \text{Eq. 11}$$

so that

$$\delta e = \frac{2R_i V_\infty \delta V_\infty}{\mu} + \frac{V_\infty^2}{\mu} \delta R_i \cdot \qquad \text{Eq. 12}$$

However, from equation 6,

$$\delta V_\infty \qquad \frac{\mu}{V_\infty R_i^2} \delta R_i \qquad \text{Eq. 13}$$

Equation 12 then becomes

$$\delta e = \frac{V_\infty^2}{\mu} \left[1 + \frac{2\mu}{V_\infty^2 R_i} \right] \delta R_i \cdot \qquad \text{Eq. 14}$$

Upon substitution, equation 10 becomes

$$\delta V_N = \frac{V_\infty}{\mu e} \frac{V_i^2}{\sqrt{e^2 - 1}} \delta R_i \qquad \text{Eq. 15}$$

where

$$\cot\alpha = \frac{\mu}{V_\infty V_i R_i} = \frac{1}{\sqrt{e^2 - 1}} \cdot \qquad \text{Eq. 16}$$

Equation 15 may be rewritten as

$$\delta V_N = \sqrt{\frac{1 + 2\xi}{1 + 1/\xi}} \cdot \frac{V_\infty}{R_i} \delta R_i \qquad \text{Eq. 17}$$

where

$$\xi = \frac{\mu/R_i}{V_\infty^2}$$

4-2. *Flight-Path Angle Error*

An error in flight-path angle will result in a shift in location of perigee and departure on a trajectory different than the design trajectory. If the path angle at injection is small, the eccentricity of the hyperbola is unchanged; the effect of such an error is to rotate the velocity vector at infinity by an angle equal to that between the nominal and actual perigee as measured from the earth's center.

Then

$$\delta V_N \sim V_\infty \, \delta \nu \qquad \text{Eq. 18}$$

where $\delta \nu$ is the angle (true anomaly) between the actual and nominal perigee of the departure hyperbola.

For small angles, the flight-path angle Γ is approximately related to the true anomaly by

$$\Gamma \simeq \frac{e}{1 + e} \, \nu \qquad \text{Eq. 19}$$

then

$$\delta \nu \simeq \frac{1 + e}{e} \, \delta \Gamma \qquad \text{Eq. 20}$$

so that

$$\delta V_N \simeq V_\infty \left[\frac{1 + e}{e} \right] \delta \Gamma = \left[\frac{2\xi + 1}{\xi + 1} \right] V_\infty \delta \Gamma \qquad \text{Eq. 21}$$

4-3. *Position Error*

If injection occurs at the wrong location in the orbit, departure from the planet is not on the nominal trajectory. To correct the resulting error in the direction of the velocity vector, an impulse only in the V_N direction is required. It is assumed that the magnitude and inertial direction of the velocity is unchanged by such an error, the departure geometry is as shown in Figure 4-2.

The angle Θ is given by

$$\Theta = \frac{1 + e}{e} \, \Psi \qquad \text{(for Ψ small)} \qquad \text{Eq. 22}$$

NOMINAL PERIGEE & INJECTION

ACTUAL LOCATION OF INJECTION

NOMINAL TRAJECTORY

ACTUAL PERIGEE

ΔV

ΔV

Ψ

ACTUAL TRAJECTORY

δx

ϕ

Θ

Ψ

δx = error in injection location

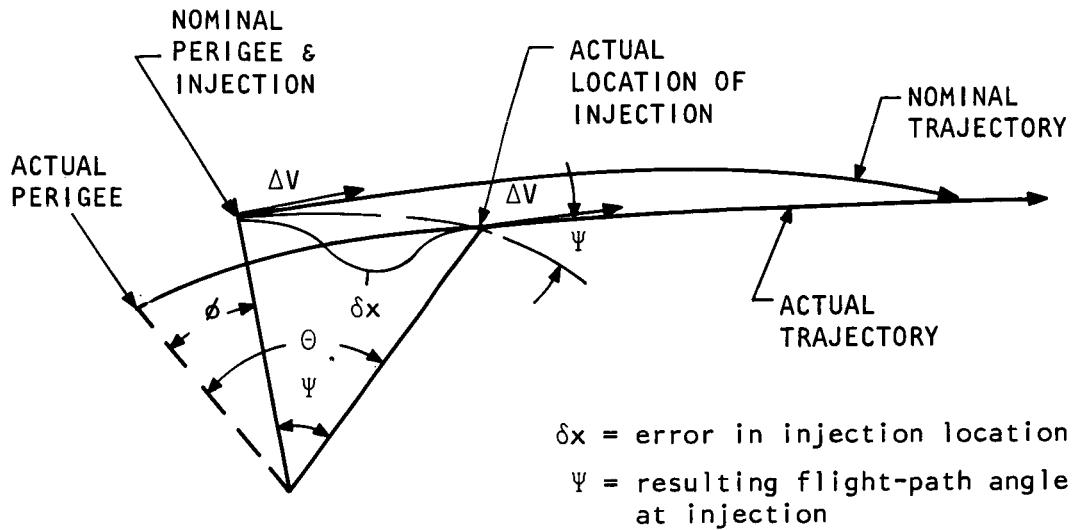Ψ = resulting flight-path angle at injection

Figure 4-2. Departure Geometry

The actual rotation of perigee is

$$\phi = \Theta - \psi = \left(\frac{1 + e}{e}\right)\psi - \psi = \frac{\psi}{e} \qquad \text{Eq. 23}$$

The velocity correction δV_N is just

$$\delta V_N = \frac{\psi}{e} V_\infty = \frac{\delta x}{e} \frac{V_\infty}{R_i} = \frac{1}{1 + 1/\xi} \frac{V_\infty \delta x}{R_i} \qquad \text{Eq. 24}$$

4-4. *Axial Errors*

Of the error sources being discussed, only errors in altitude and injection velocity also require a δV_T component of velocity to realign the departure velocity vector. Both the errors in the X and M directions require only a δV_N component to correct the trajectory. The desired δV_T partials were found as follows:

$$V_\infty^2 = V_i^2 - 2\mu/R_i \qquad \text{Eq. 25}$$

$$\frac{dV_\infty}{dV_i} = \frac{V_i}{V_\infty} \qquad \text{Eq. 26}$$

$$\delta V_\infty = \frac{V_i}{V_\infty} \delta V_i = \sqrt{1 + 2\xi} \; \delta V_i \qquad \text{Eq. 27}$$

4-7

Similarly, differentiating equation 25 with respect to R_i yields

$$\frac{dV_\infty}{dR_i} = \frac{\mu}{V_\infty R_i^2}$$

Eq. 28

4-5. *Sensitivities*

A three-dimensional view of the injection normal and axial errors is shown in Figure 4-3. The normal velocity errors caused by path angle (Γ), position (X), injection velocity (V_i), and altitude (h) errors are shown in Figure 4-4.

The parameter values used in the computation of the error sensitivities were

V_∞ = 8 km/sec,

V_i = 13.6 km/sec,

R_i = 3540 n.mi (100-nmi park orbit) or
6550 km, and

μ = 398.6 x 10^3 km^3/sec^2

The axial velocity errors (δV_T) caused by altitude and injection-velocity error are shown in Figure 4-5.
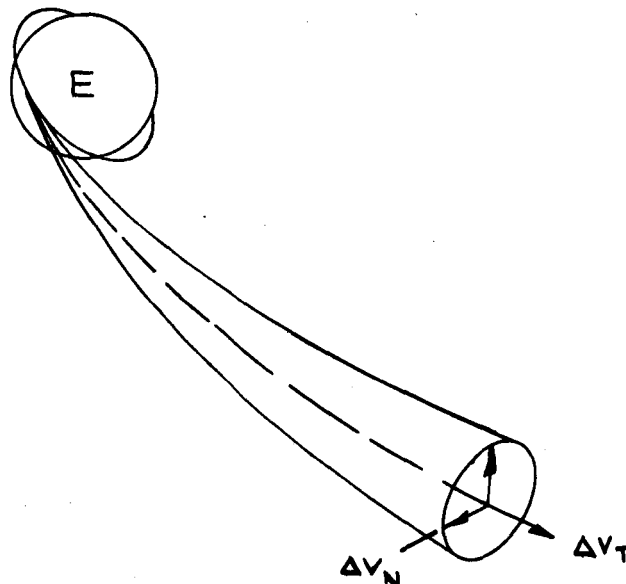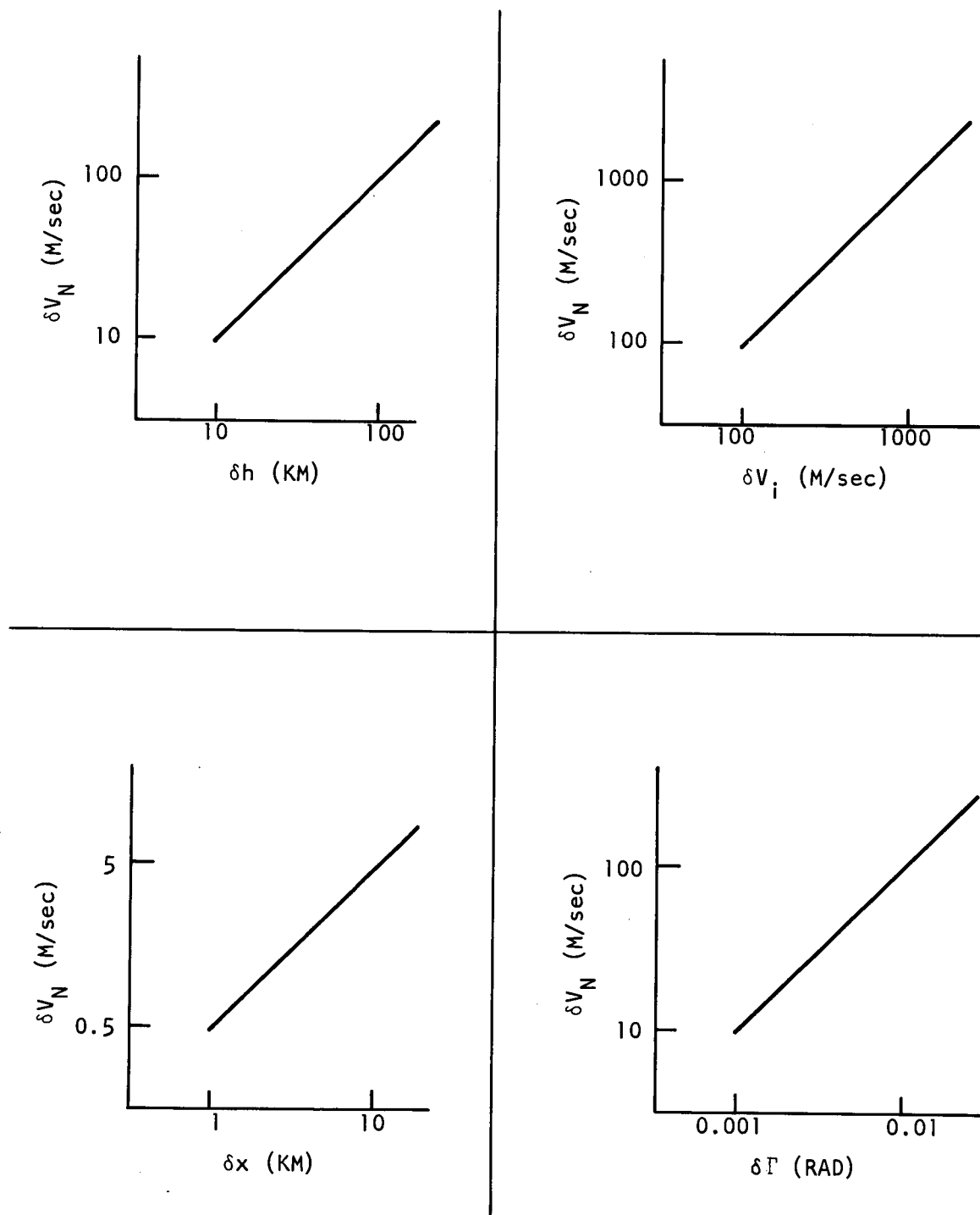

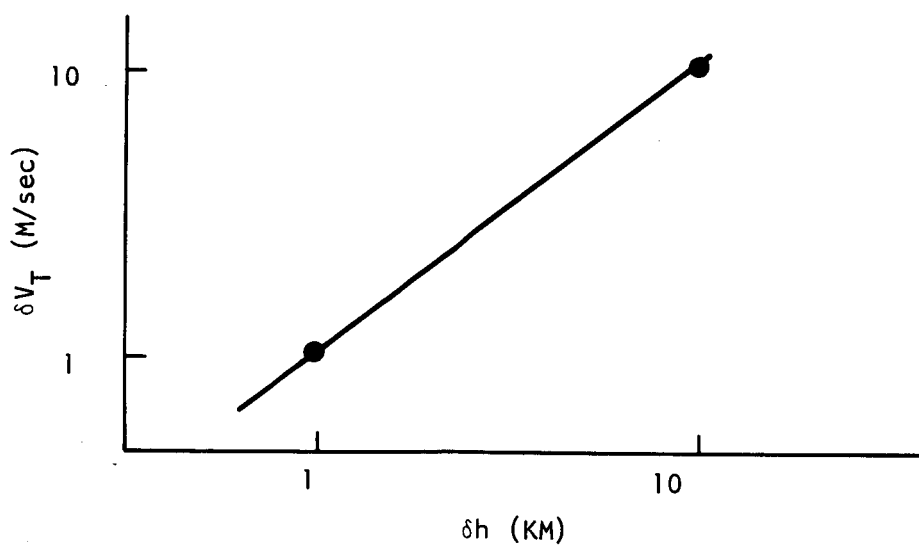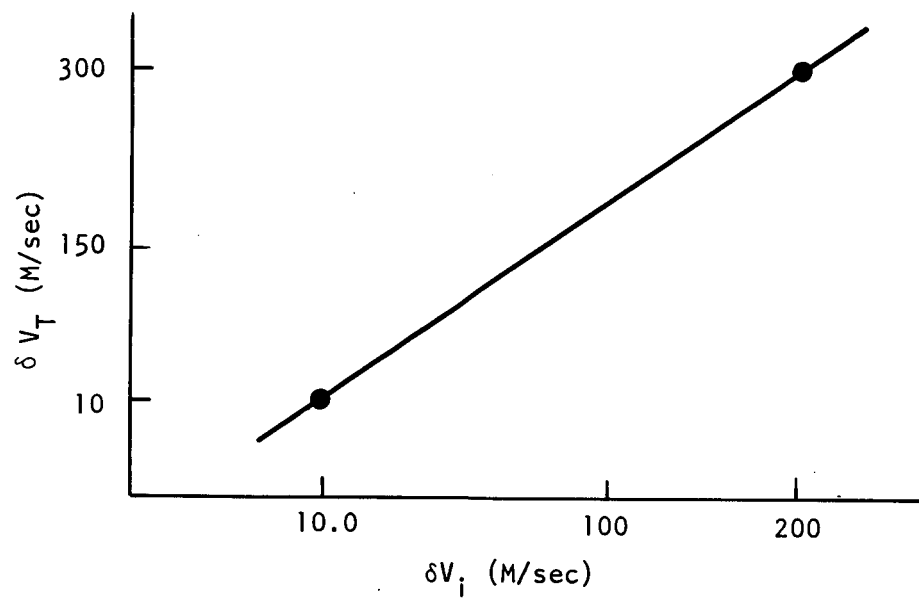Figure 4-3. *Cis-Martian Injection*

Figure 4-4. Normal Injection Errors (δV_N)

Figure 4-5. *Axial Injection Velocity Error (V$_T$)*

4-6. POST AND TERMINAL ADJUSTMENTS

As the spacecraft approaches or leaves a planet, a correction may be desired to place it into a new trajectory. As the craft approaches a planet, the geometry would appear as shown in Figure 4-6.
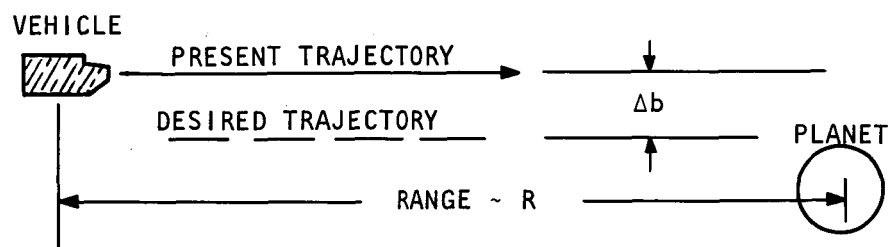
Figure 4-6. Terminal Adjustment Geometry

The minimum velocity impulse needed to deflect the spacecraft to the desired trajectory is in a direction perpendicular to the trajectory and of magnitude $\frac{\Delta b}{R} V_\infty$; the departure and arrival geometry and error sensitivities are shown in Figures 4-7 and 4-8. For a planet flyby, the planetocentric trajectory (Figure 4-9a) is hyperbolic. The direction of the departure asymptote is a function of the impact parameter, b.

A deviation in b from the nominal causes a change in Θ. The velocity impulse required to realign the velocity vector at infinity after the encounter normal to the trajectory and is given by

$$\delta \Delta V \simeq V_\infty \delta \Theta \qquad \qquad \text{Eq. 29}$$

From Figure 4-9a, it can be seen that

$$\sin \alpha = \frac{b}{\Gamma p + a} = \frac{V_\infty^2 b}{\mu} \cos \alpha \qquad \qquad \text{Eq. 30}$$

Differentiating with respect to b yields

$$\delta \alpha = \cos^2 \alpha \frac{V_\infty^2}{\mu} \delta b \qquad \qquad \text{Eq. 30}$$

4-11

a. *Geometry*

$$\Delta V = \frac{\Delta b}{R} \times V_\infty$$
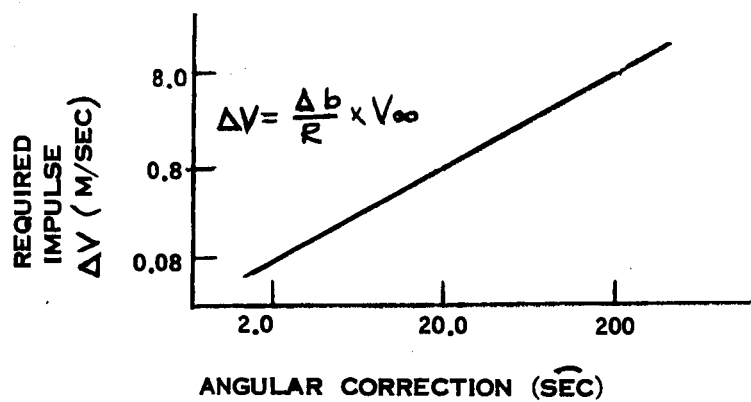
b. *Error Sensitivity*

Figure 4-7. Post-Earth-Correction Geometry and Error Sensitivity

$\dfrac{V_\infty}{\text{4.752 KM/SEC}}$

16 DAYS
R=6,640,000 KM
PLANET DISC 1$_{MR}$
1% PLANET DIAM 2 SEC

1.6 DAYS
R= 664,000 KM
PLANET DISC 10$_{MR}$
1% PLANET DIAM 20 SEC

PRESENT TRAJECTORY

Δb

DESIRED TRAJECTORY

6640KM

M

RANGE

$R_P =$

a. Geometry

$$\Delta V = \frac{\Delta b}{R} \times V_\infty$$

47.5

4.75

0.475

0.0475

REQUIRED CORRECTION, ΔV (M/SEC)

2 SEC   20 SEC   1$_{MR}$ 10$_{MR}$

ANGULAR DISPLACEMENT, $\dfrac{\Delta b}{R}$
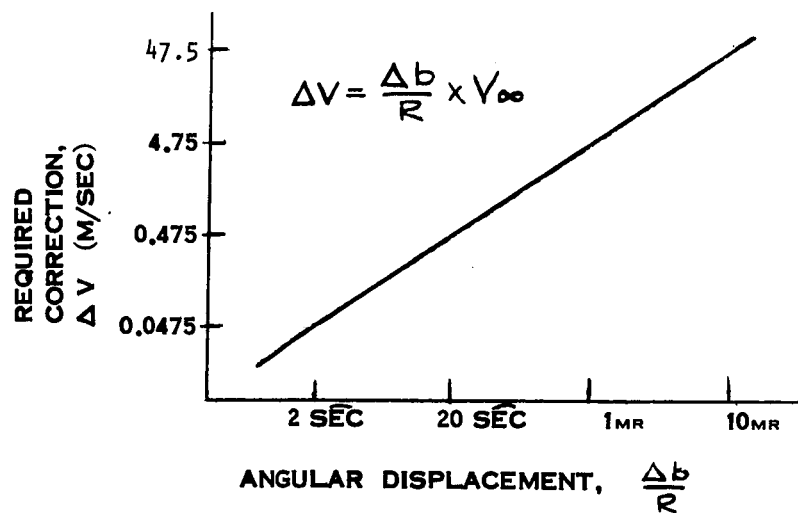
b. Error Sensitivity

Figure 4-8. Mars-Terminal-Adjustment Geometry and Error Sensitivity

$$\Delta V = \frac{2V_\infty^3}{M} \ SIN^2 \ \frac{\Theta}{2} \ \delta b$$
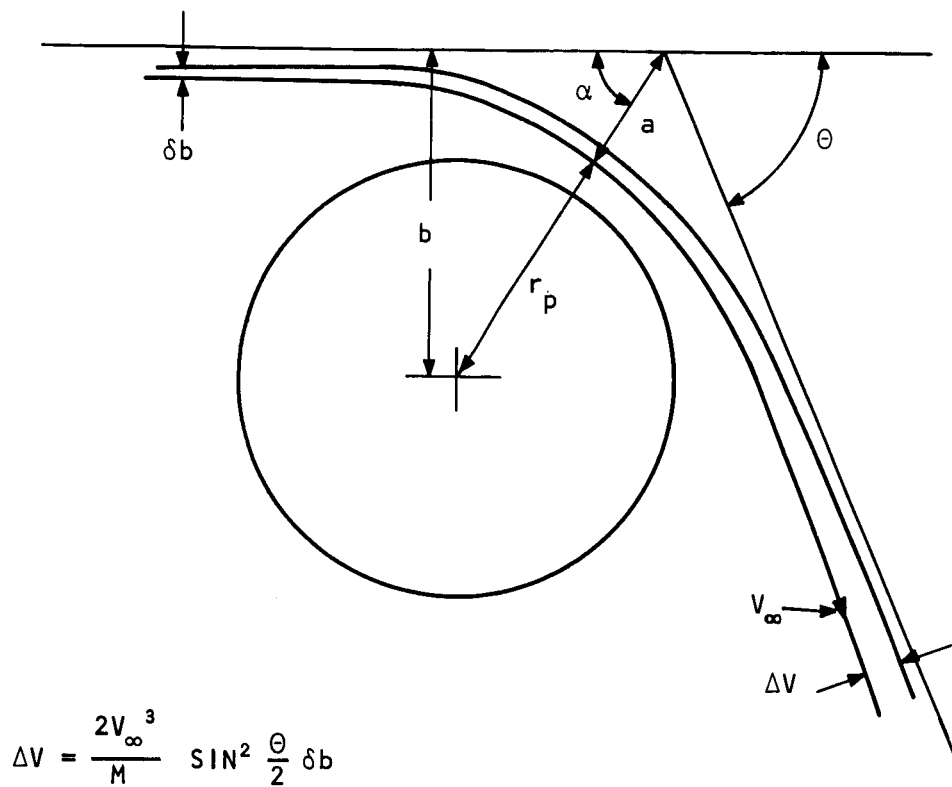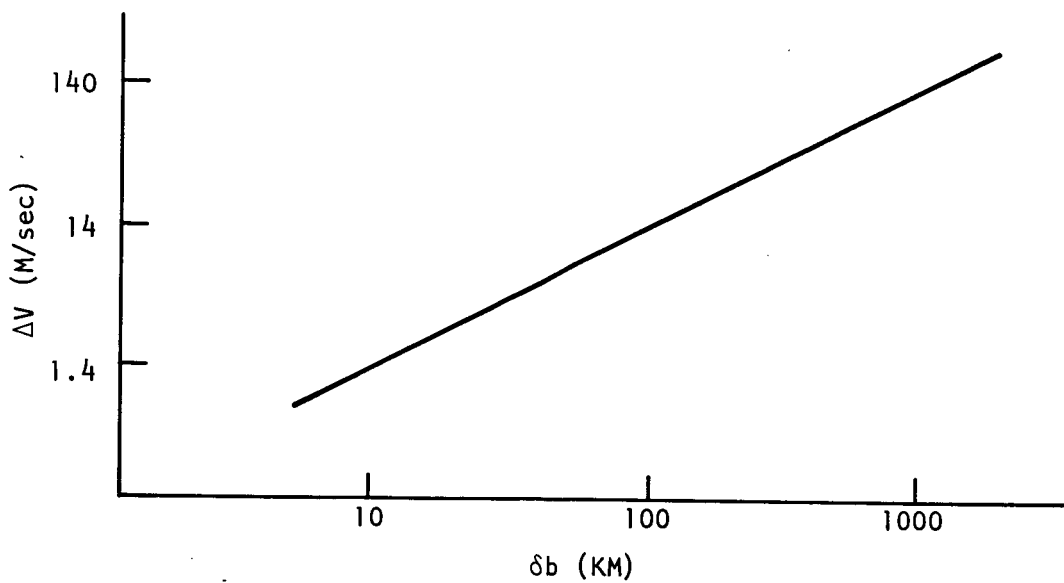
a.   Geometry

b.   Error Sensitivity

Figure 4-9.   Venus Flyby Geometry and Error Sensitivity

Since $\Theta = 180 - 2\alpha$, equation 29 reduces to

$$\delta\Delta V = \frac{2V_\infty^3}{\mu} \sin^2 \frac{\Theta}{2} \delta b \qquad \left\{ \begin{array}{l} \delta_{\Delta V} = \dfrac{2\,(167)}{325 \times 10^3} \times 0.14 \times \delta b \\[2mm] \delta_{\Delta V} \approx 0.14 \times 10^{-3}\,\delta b \end{array} \right\} \qquad \text{Eq. 32}$$

For a Venus flyby, typical values for the various parameters in equation 31 are

$$\mu\text{Venus} = 325 \times 10^3 \text{ km}^3/\text{sec}^2$$

$$V_\infty \sim 5.5 \text{ km/sec}$$

$$\Theta \simeq 45°$$

When these typical values are used, the variation of $\delta_{\Delta V}$ with δb for Θ Venus flyby is as shown in Figure 4-9b.

4-7. ORBIT ENTRY

If, as the spacecraft approaches a planet, it is desired to transfer from a hyperbolic to circular orbit, a velocity impulse of magnitude ΔV is needed to decelerate the spacecraft to circular velocity. If the altitude at which this impulse is applied is correct but an error in the magnitude of the impulse occurs, the vehicle will enter an elliptical orbit which has a perigee radius equal to that of the nominal circular orbit. An example of such an orbit for Mars is shown in Figure 4-10a.

The increase in apogee altitude over the nominal circular altitude is

$$\delta h = \frac{4R_p}{V_c} \delta\Delta V_i \qquad \text{Eq. 33}$$

The increase in apogee altitude is found from the expression

$$Ra = (1 + e)a \qquad \text{Eq. 34}$$

where   Ra = radius at apogee, and

      a = semimajor axis

or

$$\delta Ra = (1 + e)\delta a + a\delta e \qquad \text{Eq. 35}$$

4-15

a. Geometry

$$\delta h = \frac{4R_p}{V_c} \, \delta^\circ \Delta V_i$$
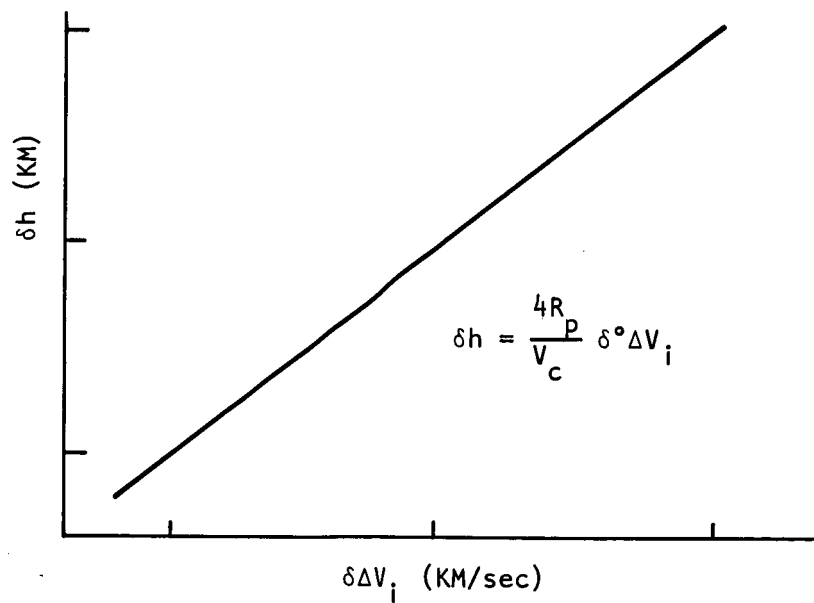
b. Error Sensitivity

4-10. Mars Entry Geometry and Error Sensitivity

Because the perigee radius does not increase, an expression for a can be found:

$$R_p = a(1 - e) \qquad\qquad \text{Eq. 36}$$

$$\delta R_p = 0 = \delta a(1 - e) - a\delta e \qquad\qquad \text{Eq. 37}$$

or

$$\delta Ra = 2\delta a \qquad\qquad \text{Eq. 38}$$

The semimajor axis is given by

$$\frac{1}{a} = \frac{2}{R} - \frac{V^2}{\mu} \qquad\qquad \text{Eq. 39}$$

Differentiating with respect to V yields

$$\frac{da}{a} = \frac{2}{\mu} \, aV^2 \, \frac{dV}{V} \qquad\qquad \text{Eq. 40}$$

or

$$\delta Ra = 4a \left(\frac{aV^2}{\mu} \right) \frac{dV}{V} \qquad\qquad \text{Eq. 41}$$

If the nominal orbit is curcular, the following relations obtain:

$$\frac{aV^2}{\mu} = 1, \qquad\qquad \text{Eq. 42}$$

$$a = R_p, \qquad\qquad \text{Eq. 43}$$

and

$$V = V_c \qquad\qquad \text{Eq. 44}$$

Thus,

$$\delta h = 4R_p \, \frac{dV_i}{V_c} \qquad\qquad \text{Eq. 45}$$

For a "typical" Mars flight,

$$R_p = 4300 \text{ km}$$

$$V_c = \sqrt{\frac{\mu}{R_p}} = 3.0 \text{ km/sec for h} \sim 1000 \text{ km}$$

Using these values, the relation of δRa with δV_i is as shown in Figure 4-10b.

4-17

4-8. SUMMARY

The derived error-sensitivity curves for cis-Martian injection show that for moderate altitude (10-km), position (10-km), path-angles (1-mΓ), and injection-velocity (10-m/sec) errors, the resulting normal velocity (δV_N) errors will be approximately 12 m/sec or less. The axial-velocity errors, δV_T, are 17 m/sec or less for altitude and injection-velocity errors of 10 km and 10 m/sec, respectively.

Post- and terminal-adjustment errors are directly related to the post- and terminal-trajectory angle errors. Therefore, for a hyperbolic excess velocity of 8 km/sec, the required trajectory velocity correction will be less than 10 m/sec for a milliradian error. Measurement accuracies of 20 arc-seconds will hold the correction error to less than 1 m/sec.

The accuracy of the Venus flyby angle is a function of the trajectory displacement error. A trajectory displacement error of 100 km in Venus flyby will require a velocity impulse of less than 15 m/sec δV.

Orbital-entry injection-velocity errors are extremely serious. For example, a 10-m/sec, δV, error will result in approximately an 80-km δh error at the 180-degree orbit phase point.

SECTION 5
NAVIGATION AND GUIDANCE

The navigation and guidance functions of a manned mission to Mars, and return by way of Venus, can be accomplished using a wide variety of techniques. This section discusses the navigation and guidance information requirements and general methods that will satisfy the navigation and guidance requirements of the manned Mars mission.

Two basic approaches will be considered: the "semiautomatic" approach requires only a moderate amount of manual operation; the "aided-manual" approach is more manual in concept. The consideration of two basic approaches does not mean that one or the other would be selected; elements of both approaches probably would be incorporated into the equipments selected for a Mars mission.

Semiautomatic and Aided-manual approaches will be discussed for orbit determination, injection, post and terminal adjustment, orbit entry, and station-keeping mission phases.

In general, the crew can participate in all navigation and guidance activities, including obtaining basic data, processing data, and guiding the vehicle. The *extent* of man's contribution, however, varies in the two approaches.

5-1. ORBIT DETERMINATION

The parameters that must be obtained to identify and adjust planetocentric orbit are orbit size and shape, orbit orientation in the celestial sphere, and the position of the vehicle in the orbit as a function of time. The size and shape of the orbit may be expressed in terms of eccentricity and the major or minor axis. The orientation of the orbit may be expressed by a set of direction cosines or Euler angles defining a line normal to the orbital plane. The orientation of the

orbital elipse in the orbital plane can be stated as an angle measured from the ascending node. Orbital vehicle position at any time can be expressed as an angle from some fixed point on the orbit, such as the ascending node, or periapsis.

5-2. *Orbit Geometry*

Figure 5-1 illustrates the geometry of an earth-centered coordinate system and the optical observations required to determine the orientation of the orbital plane. The observations consist of measuring a latitude star-horizon angle (L_a), and a longitude star-horizon angle (L_N) (Figure 5-2). The orbital shape and major axis orientation within the orbital plane is determined by vehicle altitude measurements.

5-3. *Semiautomatic Orbit Determination*

Figure 5-3 shows the data-acquisition information flow for a semiautomatic orbit-determination approach. The optical instrumentation could consist of a horizon scanner and a star tracker; these instruments would provide data from which the latitude and longitude star-horizon angles could be obtained. An instrument is also required to provide ranging or altitude information.

The sequence of principal operations for a semiautomatic approach to orbit determination is as follows:

1. The IMU is operated in the gimbaled stabilization mode with stellar drift correction from the star trackers to provide a stabilized plane nominally parallel to the orbital plane.

2. The vehicle is rotated about an axis normal to the nominal inertial orbital plane by use of the horizon-scanner local vertical data.

3. Gyrocompassing is used to determine the normal to the orbital plane.

4. Inertially derived orbital-plane calculations are verified and corrected by stellar gyrocompassing. The star-orbit plane angle will cone unless the star offset line of sight is normal to the orbital plane.
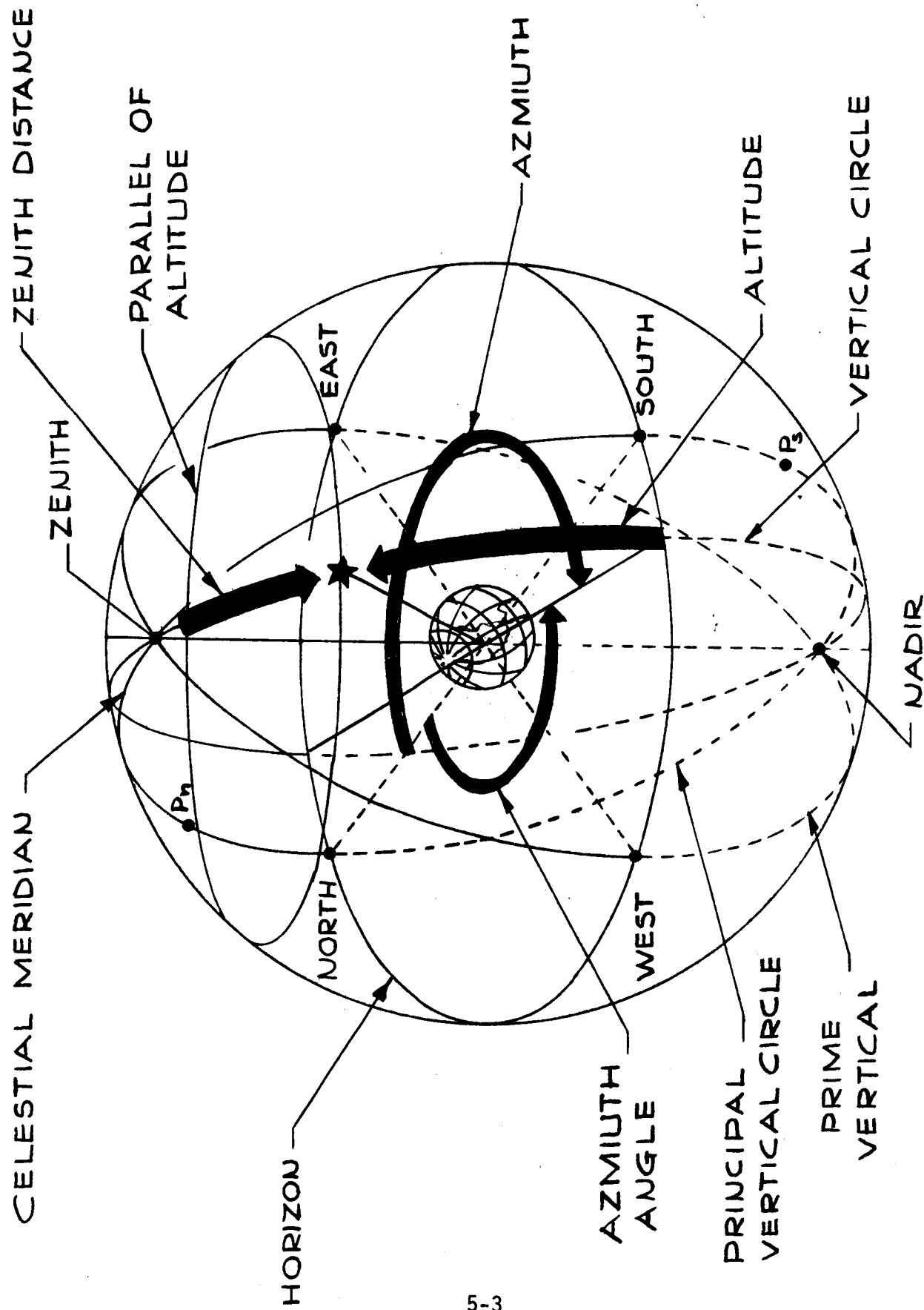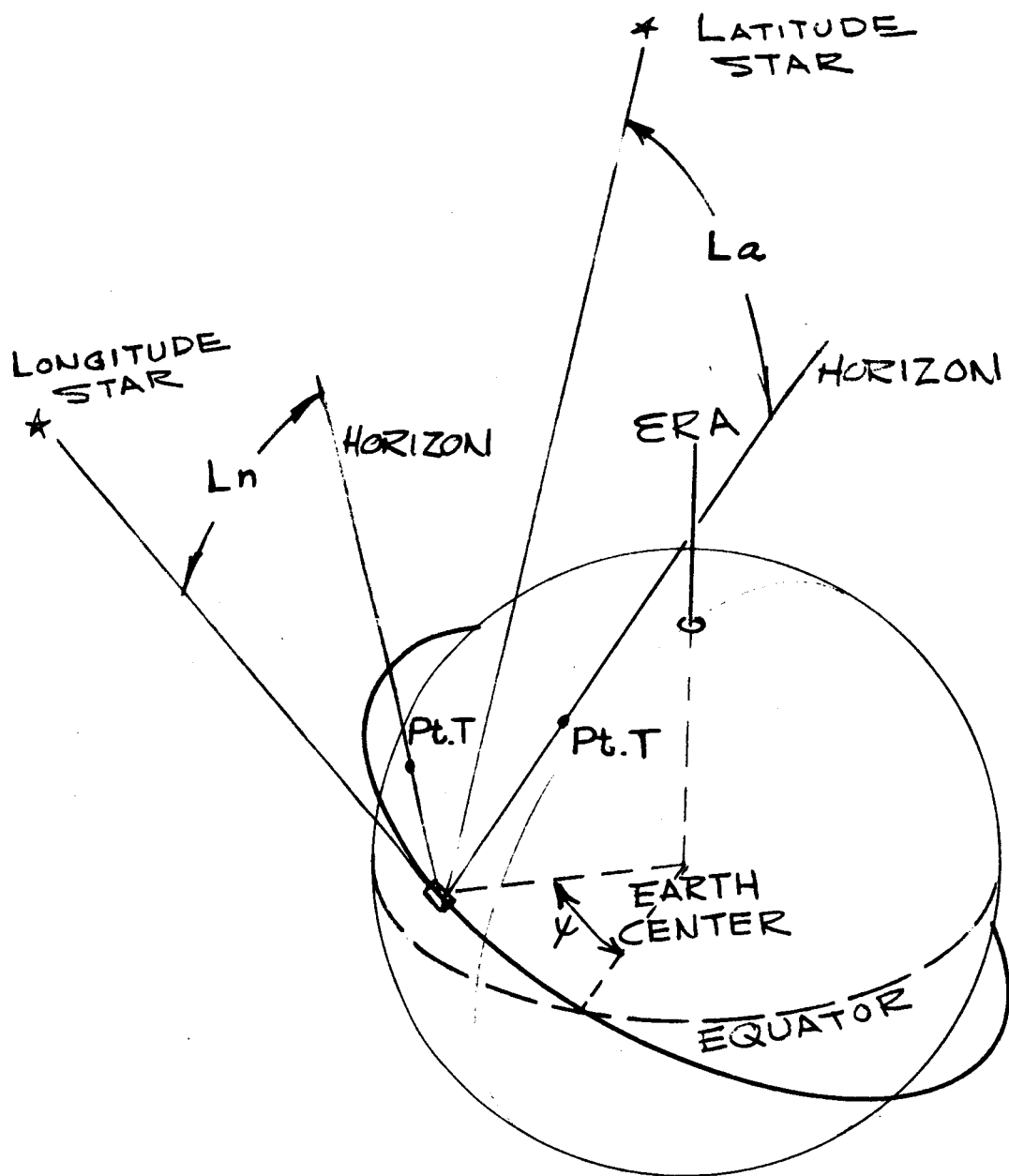
Figure 5-1. Horizon System of Coordinates

5-3

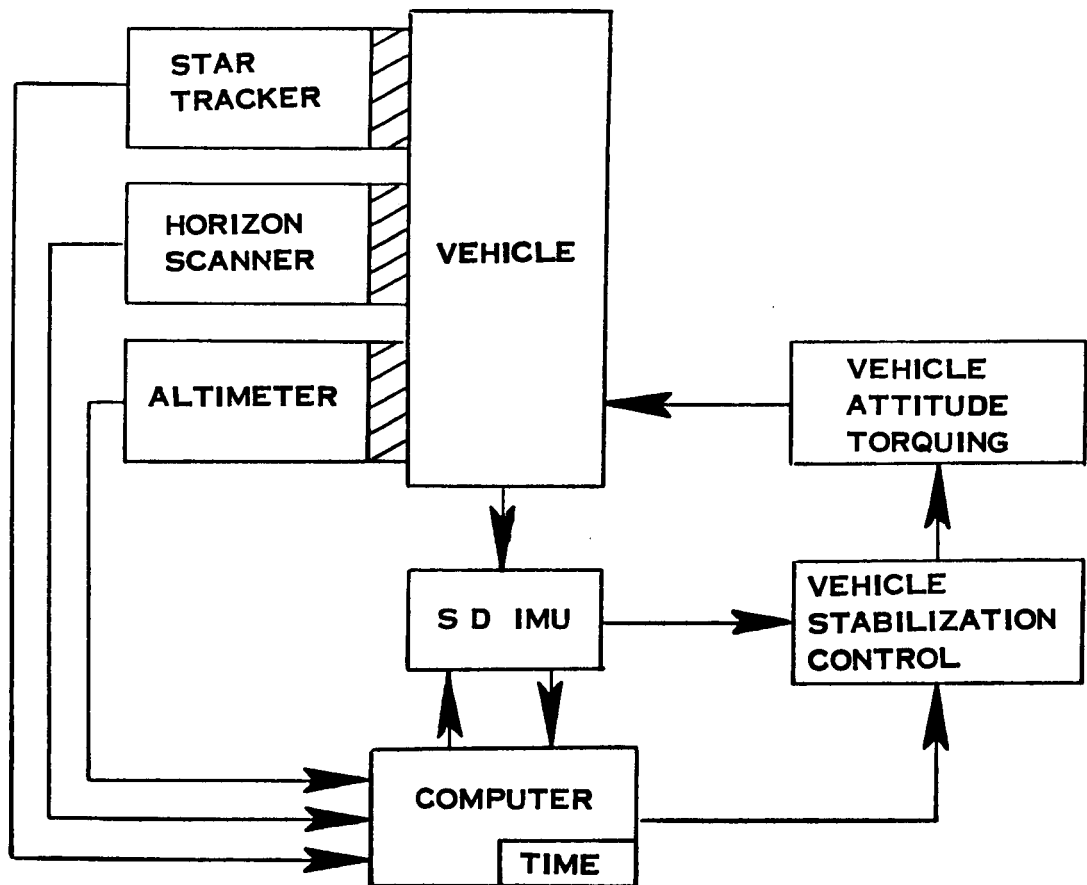Figure 5-2. Space-Sextant Measurement Geometry

Figure 5-3. A Method of Semiautomatic Orbit Determination

5. Planetocentric position measurements are now obtained by the automatic equivalent of conventional celestial marine navigation through use of the horizon scanner and star trackers, and computer-supplied time.

6. Orbital height is obtained from the automatic altimeter data.

7. Final orbit calculations are made by the computer, which weighs the various inertial planet and stellar data to provide the best estimate of the planetocentric orbit.

5-4. *Aided-Manual Orbit Determination*

Figure 5-4 is a data-acquisition and information-flow diagram for an aided-manual orbit determination. Optical data are supplied by a sextant and a stadimeter. The sextant provides direct measurements of the latitude and longitude stars (Figure 5-2), and the stadimeter is used to provide altitude data. These instruments are described in Section 6.

The sequence of principal operations for aided-manual orbit determination is as follows:

1. The vehicle is brought to the proper attitude for navigational observations.

2. The vehicle is maintained at this attitude to keep the optical targets within the sensor field in view. Methods of accomplishing manual attitude control required for navigational observations are discussed in Section 6.

3. A series of stadimeter sightings are taken to obtain altitude data.

4. Smoothed stadimeter data is used to compute the orbital elements which determine orbit size and shape.

5. A series of sextant sightings are taken to obtain a number of star-horizon angle pairs at various points in the orbit.

6. The sextant data are used to determine the orbital elements which fix the plane of the orbit and the position of the vehicle in the orbit as a function of time.

5-5. *Orbit Correction*

Having determined the orbit, the next step is to correct the orbit so that it lies in the plane of the preselected cis-Martian
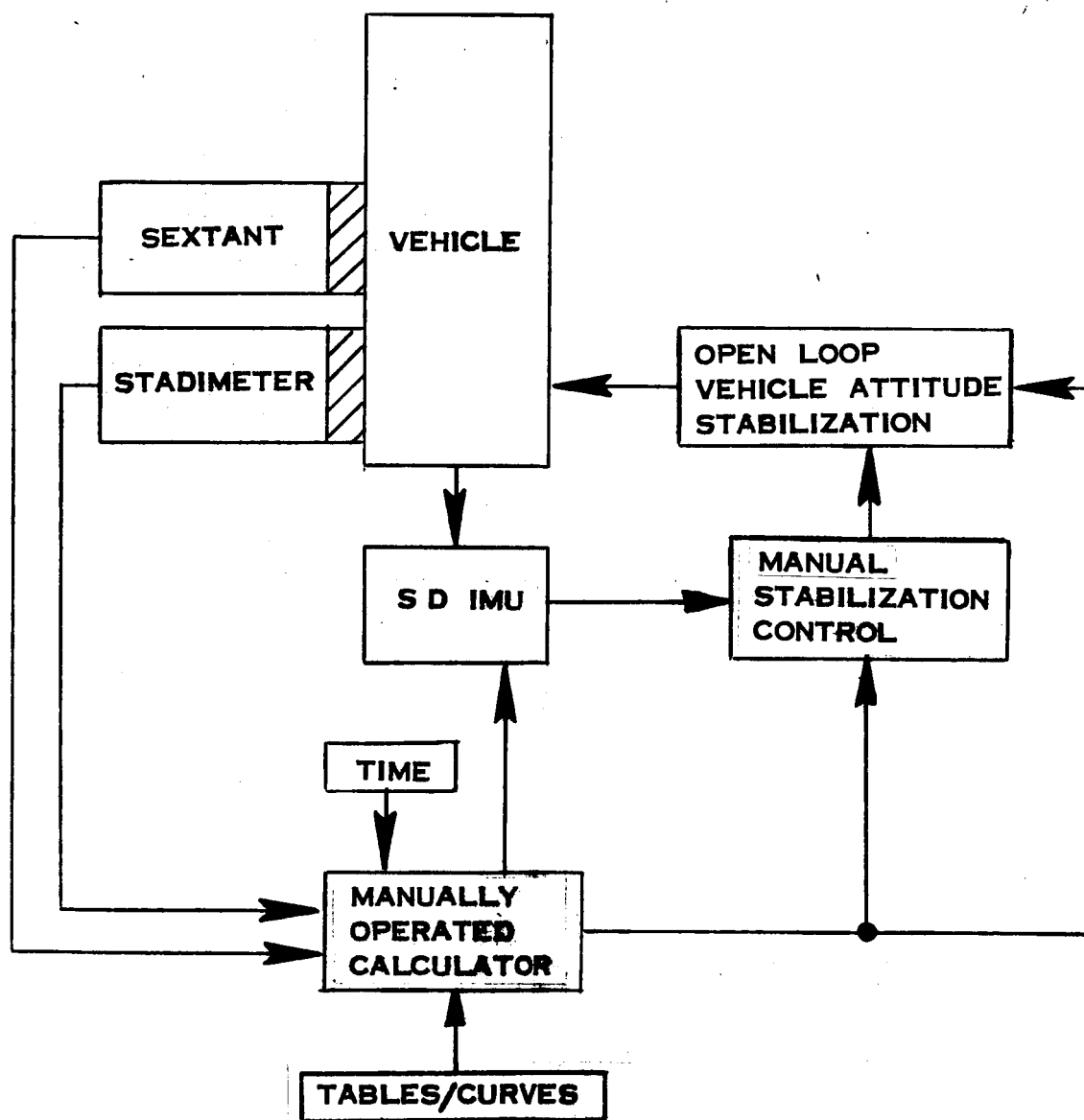
Figure 5-4. A Method of Aided-Manual Orbit Determination

trajectory. Since the techniques and procedures for correcting the orbit are essentially the same as those for other guidance events, this function will not be discussed here. For the purposes of this study the major difference between orbit correction and other guidance events is the computation requirements. These will be discussed in detail in the Phase II report.

5-6. INJECTION

The injection of a space vehicle orbiting a planet into a heliocentric transfer to another planet requires the application of an impulse of velocity to the spacecraft at the proper point in its planetocentric orbit. A heliocentric cis-Martial orbital geometry is shown in Figures 5-5 and 5-6. The orbit passes through a plane determined by three points: the Earth's position at launch, the Sun, and the position of Mars at arrival. This plane may be defined by a set of direction cosines which analytically fix the normal to the orbital plane, the inclination angle of the orbit plane to the ecliptic plane, and the angular location of the intersection of the orbital plane with the ecliptic plane.

The cis-Martian injection velocity for the base-line trajectory is 13.62 km/sec and the excess hyberbolic velocity reaches a value of 8.02 km/sec as the vehicle departs from the earth.

The navigational and guidance requirements of injection can be divided into two steps. The first step consists of determining the correct planetocentric position and proper heliocentric orientation, and determining the required ΔV. The second step consists of achieving and maintaining the correct attitude during the injection-impulse engine burn. A mission timing is assumed which places the vehicle in the correct heliocentric position.

Planetocentric position as a function of time is obtained from the previous orbit determination phase. From this data, and on the basis of a precomputed cis-Martian trajectory, the time of impulse and

V_{MAR} = 21.975 KM/SEC
V_P = 19.88 KM/SEC
V_{HP_∞} = 4.752 KM/SEC

R_P

249.2 x 10⁶ KM

628.9 x 10⁶ KM

R_L
151.9 x 10⁶ KM

E

LAUNCH DATE — JULY 24, 1977
FLIGHT TIME — 252 DAYS
ARRIVAL — APRIL 2, 1978

V = 29.318 KM/SEC
V_L = 32.8 KM/SEC
V_i = 13.62 KM/SEC
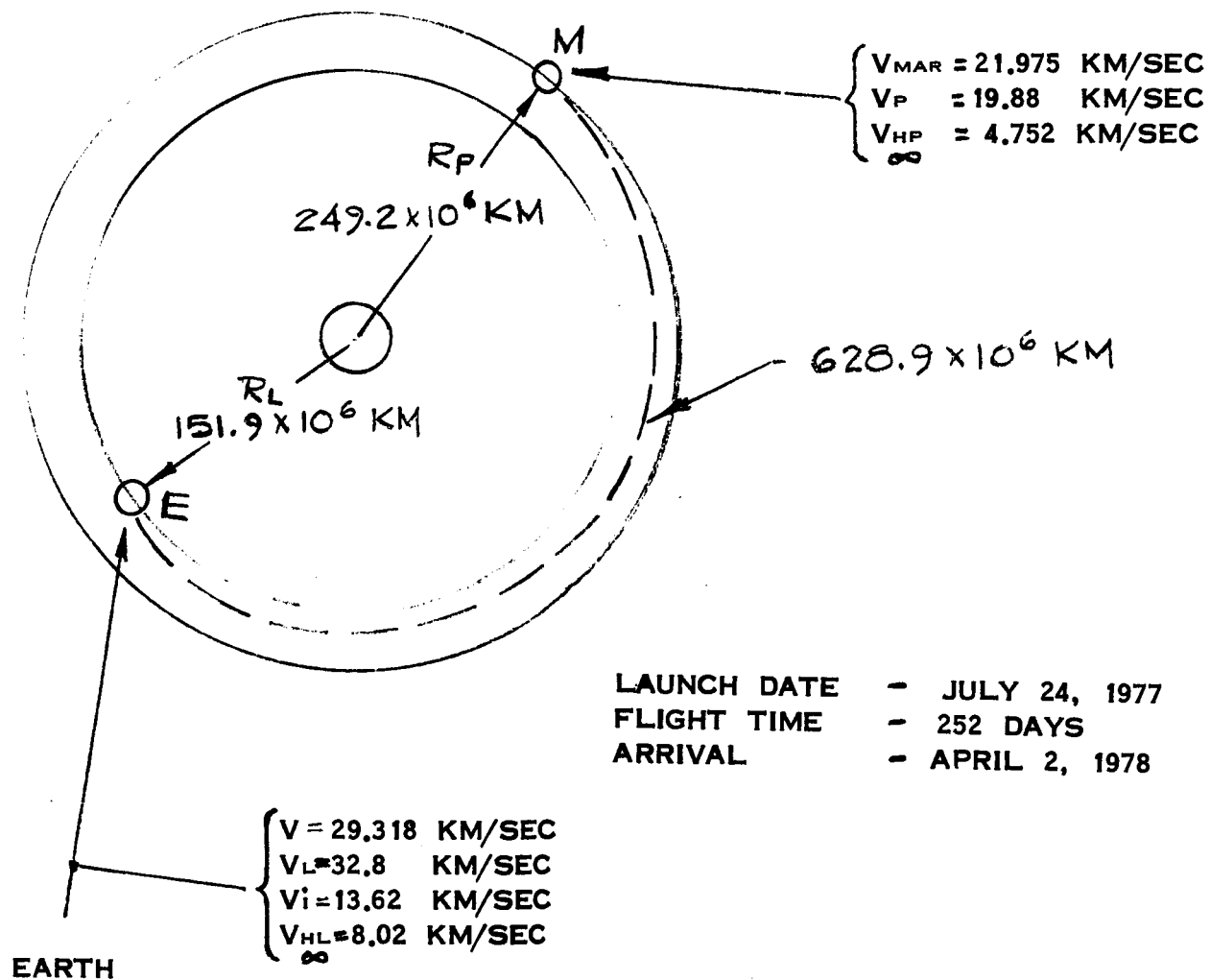V_{HL_∞} = 8.02 KM/SEC

EARTH

Figure 5-5. Geometry of a Cis-Martian Orbit
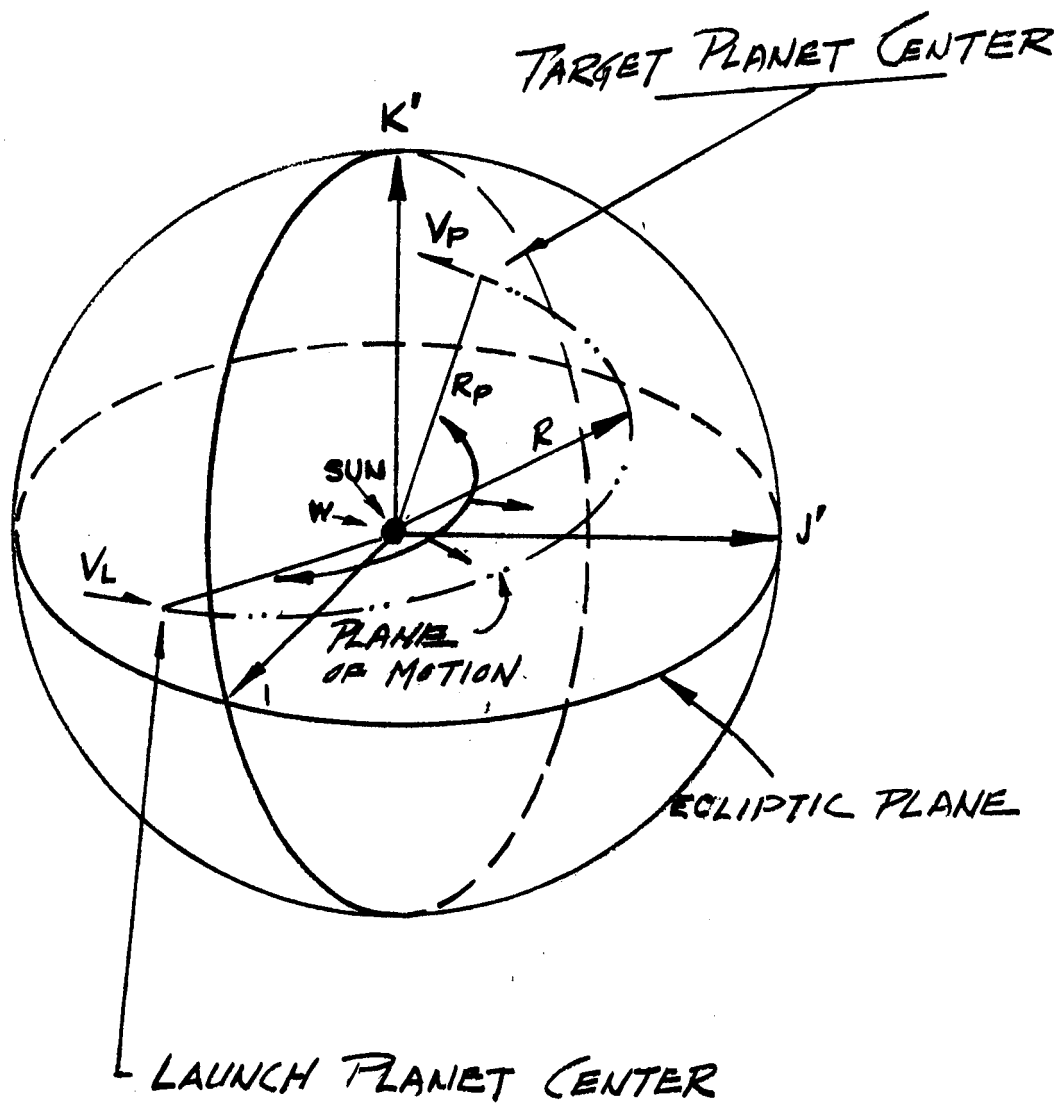
Figure 5-6. Heliocentric Transfer Geometry

the ΔV may be computed. The vehicle orientation or attitude within the celestial sphere for thrusting may be expressed in terms of two stars measured relative to a stable reference frame. This is a pre-computed direction based on the nominal earth orbit. If the stars selected are within several degrees of the desired vehicle-injection attitude, the geometry is simplified as shown in Figure 5-7. This figure shows orientation of the injection-velocity impulse (nominal star track reference) and two stellar attitude references. The injection alignment error is shown as the difference between the injection target attitude and the vehicle star tracker reference. Proper mechanization of the injection phase requires a guidance which utilizes this difference to minimize the error between the velocity impulse attitude and the injection target attitude.

5-7. *Semiautomatic Injection*

Figure 5-8 illustrates the data acquisition and information flow for a generic semiautomatic cis-Martian injection approach.

The first step of the injection phase, determining the proper time, attitude and impulse, is accomplished by the on-board computer.

The second step of the injection phase, applying the required thrust, is accomplished by the following equipment:

> 2-2 axis star tracker (attitude),
>
> Horizon scanner (local vertical),
>
> Altimeter (altitude),
>
> Time reference,
>
> Computer,
>
> Vehicle stabilization subsystem, and
>
> Inertial navigation and guidance system.

The inertial navigation and guidance system could consist of a strap-down inertial measuring unit (SD IMU) a computer, vehicle-stabilization control, vehicle attitude torquing, and an engine with associated ignition, cutoff, and gimbaling.

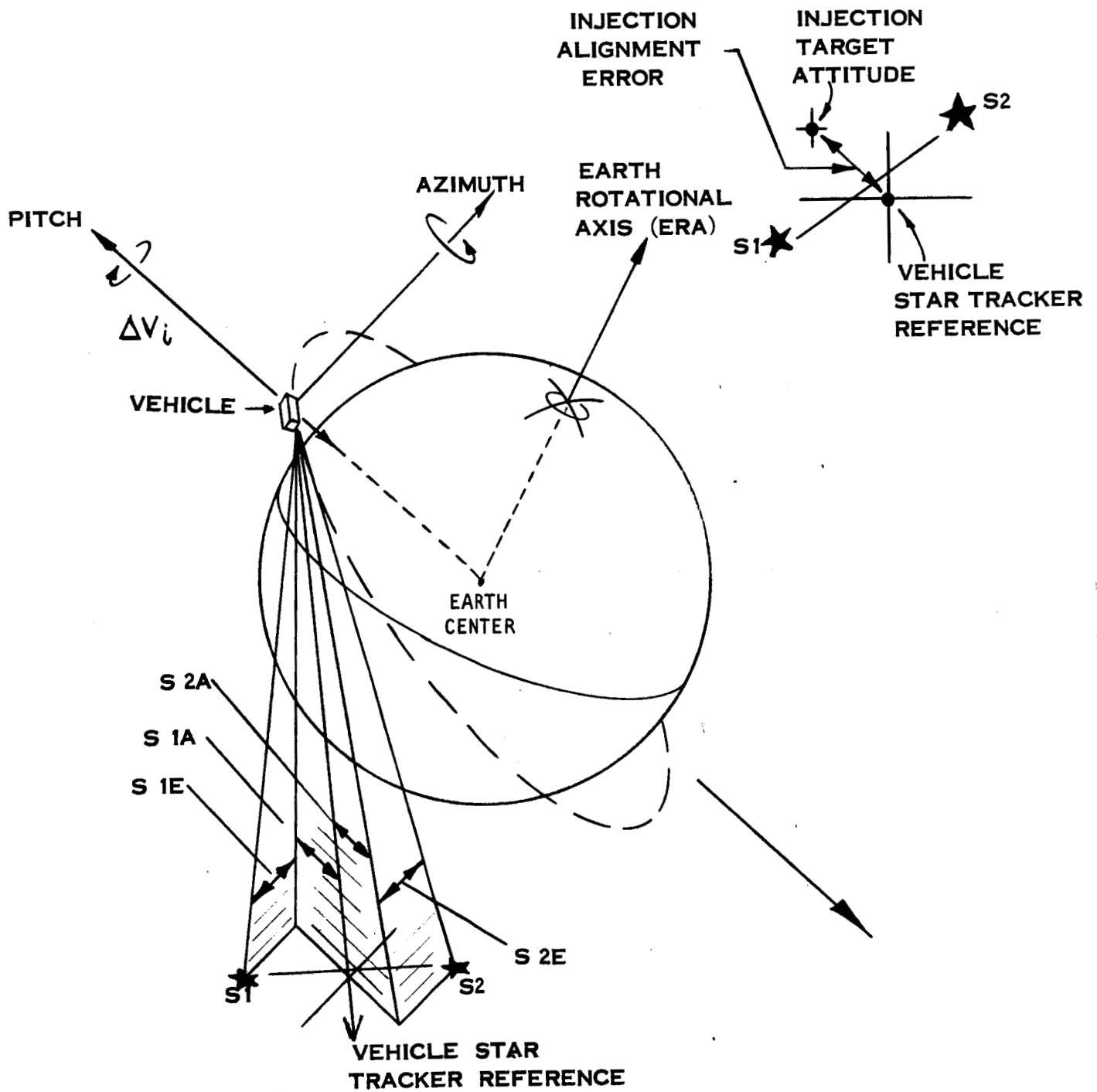Figure 5-7.   Cis-Martian Injection Star Tracker Alignment
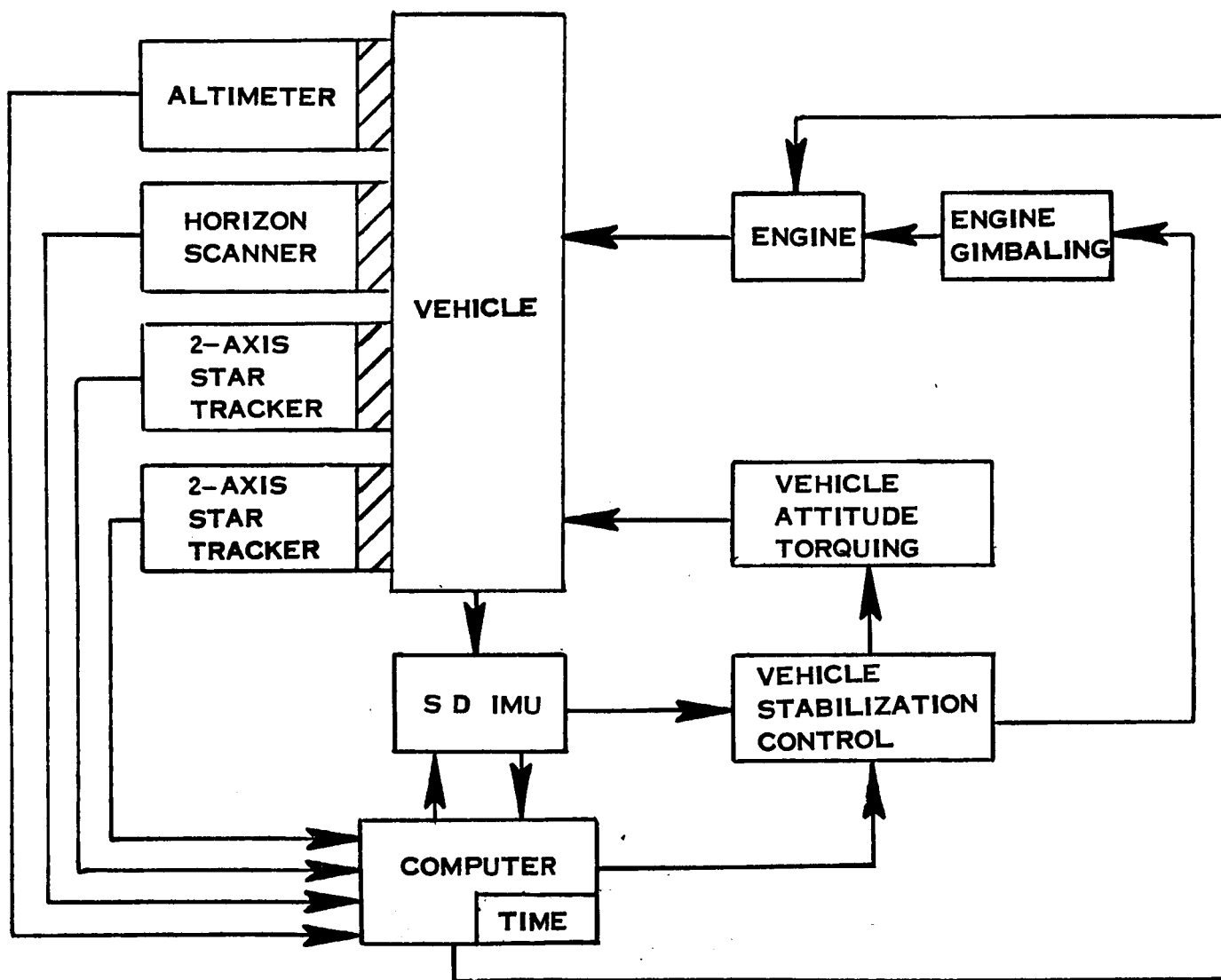
Figure 5-8. Semiautomatic Cis-Martian Injection

Navigation and guidance requirements for this phase are a two-step process. To initiate and terminate the burn at the proper time, the crew will use information brought from earth and previously calculated during the planet orbit phases.

The nominal trajectory on which the mission is based will define the orbit from which the vehicle should inject, the time of injection, the burn time, and the celestial attitude which should be held during the injection process.

Orbit-determination processes already completed will enable the crew to determine any changes which are required; however, once the earth-orbit plane is corrected, only two adjustments need be made—turn-on time or burn time. The former is most likely and would be used to compensate for the effect of improper orbital altitude which, if it were other than nominal, would change the time when the vehicle arrived over the ground track point which represented the proper on-time.

Since the vehicle would not pass over this point if the angle of inclination of the orbit were other than nominal, this condition would be compensated for by a slight variation in celestial attitude and an increased burn time.

The injection would then involve the following operations:

1. The vehicle attitude stabilization system is set to proper injection attitude.

2. Star trackers are aligned with selected stars (1 and 2 in Figure 5-7).

3. The vehicle is oriented to minimize the injection alignment error.

4. The vehicle is placed in the gimbaled inertial stabilization mode with stellar updating providing inertial drift correction.

5. Engine ignition is commanded when the vehicle reaches the correct planetocentric position.

6. The vehicle is then placed in a navigation-and-guidance mode to measure and control the applied injection-velocity vector (ΔV_i); during engine burn, the navigation-and-guidance system controls engine gimbaling, vehicle attitude, and engine cutoff.

The operational complexity of the instrumentation is considerably reduced by the introduction of man into the system. Man is available to provide control for operation sequencing, to make decisions when there is ambiguity in discrimination, to replace pattern-recognition devices, and for memory functions.

5-8. *Aided-Manual Injection*

Figure 5-9 illustrates the data acquisition and information flow for a generic aided-manual cis-Martian injection. As previously noted, the first step of the aided-manual injection, determining engine turn-on time and ΔV, is directly derived from the orbital phases and can be accomplished manually with the aid of tables and a simple arithmetic calculator.

The proper vehicle attitude for injection may be attained and maintained by use of a wide-angle (5 degrees) manually pointed star tracker which provides a view of several injection-alignment stars, the injection direction, and the injection-alignment error. With the use of the alignment-error presentation (described in Section 6), a crew member can manually adjust the vehicle attitude torquing to minimize alignment error.

The cis-Martian injection will utilize a comparatively high thrusting level and, consequently, require a high activation response and correct error interpretation for the proper guidance of the space-craft. The practicality of manual control would be improved if the injection-impulse duration were increased, and thus the total change in velocity were made over a longer time, so that the effect of mis-alignments were less critical.

The manually controlled injection could consist of the following grouping of equipment:

> Wide-angle star tracker,
> Integrating accelerometer (part of SD IMU),
> Manual engine igintion-and-cutoff subsystem,
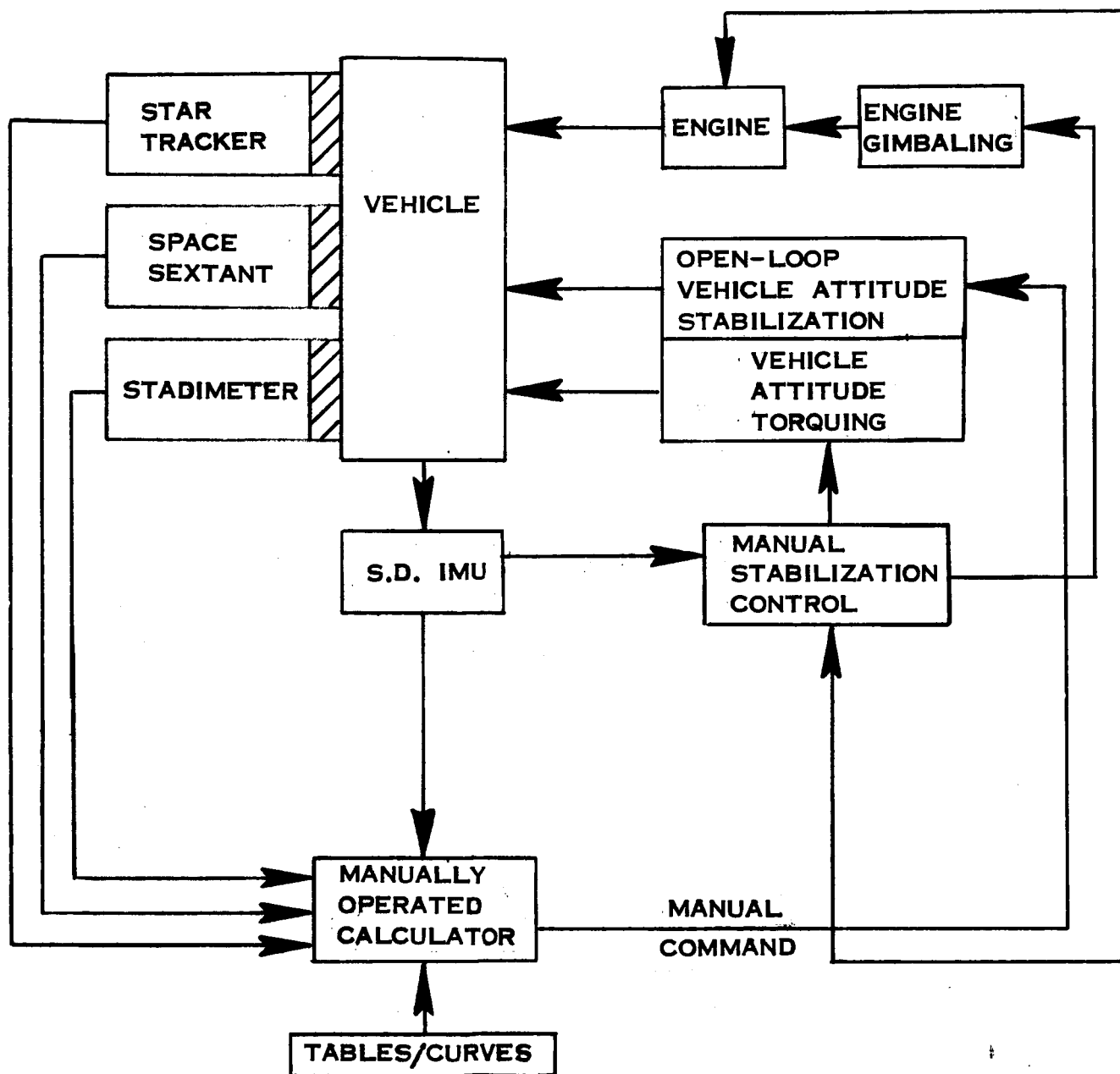
Figure 5-9. *Aided-Manual Cis-Martian Injection and Orbit Entry*

Open-loop vehicle-attitude-stabilization subsystem,

Vehicle-attitude torquing, and

Moderate-thrust injection engine.

In this navigation-and-guidance configuration, the wide-angle star tracker provides pointing-error information, which is used to determine the manual vehicle attitude torquing required to maintain proper vehicle orientation.

Components normal to the desired line of thrust or velocity impulse may be corrected by observing a display of the normal output of the IMU and manually nulling the normal integrated impulse by gimbaling the thrust engines, or by adding normal thruster impulses.

Engine cutoff will be executed when the in-line integrated acceleration measured by the IMU's accelerometer reaches the desired injection ΔV.

The sequence of principal operations for the aided-manual injection is as follows:

1. The crew member manually controls the vehicle-attitude stabilization subsystem to the proper injection orientation relative to the celestial sphere.

2. Manual servocontrol of the vehicle-attitude stabilization subsystem is maintained by monitoring injection-alignment error on the wide-angle star tracker.

3. Engine ignition is manually commanded at the time precalculated for the correct planetocentric position.

4. Manual guidance may be performed by "flying" the space vehicle along the predetermined injection-star alignment path. Flying the spacecraft consists of manually controlling the vehicle attitude for proper orientation. The engine may be manually gimbaled or normal thrusters activated to minimize any accrued velocity normal to the preselected injection attitude.

5. Engine cutoff is manually executed when the in-line integrated acceleration reaches the requisite injection velocity.

5-9.   POST AND TERMINAL ADJUSTMENT

Post and terminal adjustment of interplanetary trajectories will be required at many points in the mission. These adjustments will be

performed 1 to 20 days after leaving or before arrival, at the gravitation influence of a planet. The purpose of these adjustments is to ensure a correction of the injection errors before the error buildup becomes excessive. Post-Earth correction geometry and Mars terminal-adjustment geometry were presented in Figures 4-7a and 4-8a, respectively; the line-of-position geometry for Earth-departure trajectory, and solar-position-fix geometry are shown in Figures 5-10 and 5-11, respectively.

Post and terminal adjustments may be effected by the near-planet line-of-position approach or the solar-position-fix approach. The data required for a solar-position fix is two sun-star measurements and one planet-sun measurement. The geometry of the solar-position fix is shown in Figure 5-10. Geometrically, the two sun-star measurements form two conics with their conic axis along the sun-star line and conic intersection along the sun-space vehicle line of sight. Measurement of the sun-planet angle provides sufficient data to solve the sun-planet-vehicle triangle and obtain the vehicle's solar position. The above method is described in detail in Battin (1964).

The near-planet approach described below has the advantages of providing comparatively high accuracy coupled with simplicity, while the solar-position-fix approach provides data from which absolute solar position may be calculated. The error in the solar-position calculation is not particularly sensitive to the midcourse region in which the measurements are made; however, it apparently is not as accurate as the near-body approach, even though the near-body measurements are limited to a period of 1 to 20 days distance from a planet. The solar-fix approach could be used to check navigation during the midcourse trajectory.

5-10. Near-Planet Line-of-Position Approach

The near-planet line-of-position approach consists of determining the attitude of the vehicle-planet line of sight by comparing it with known attitudes of adjacent stars. Figure 5-10 shows an observer taking a near-planet/star view, and visually measuring an elevation and azimuth angle.
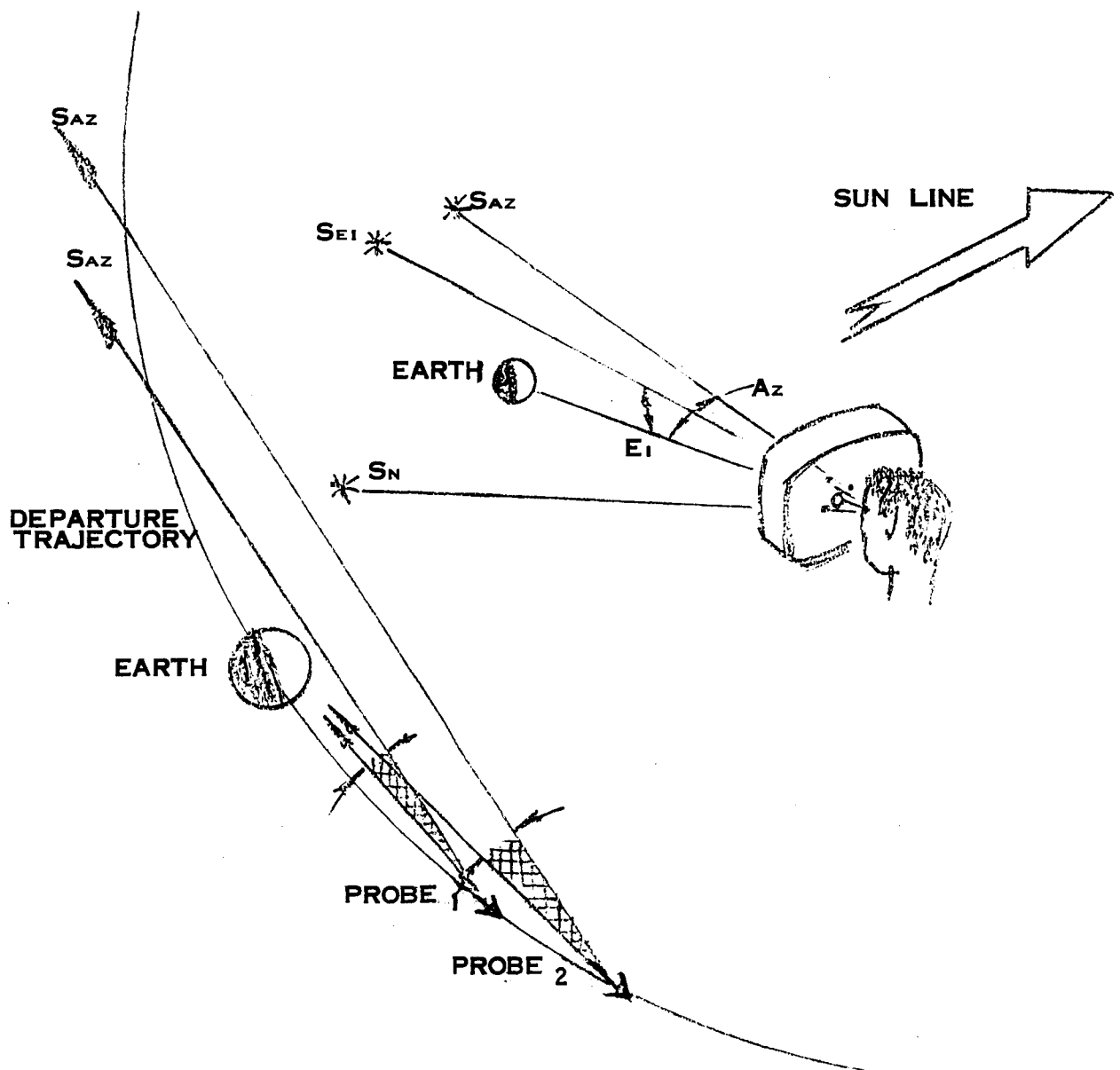
Figure 5-10. Earth-Departure Trajectory Line-of-Position Geometry
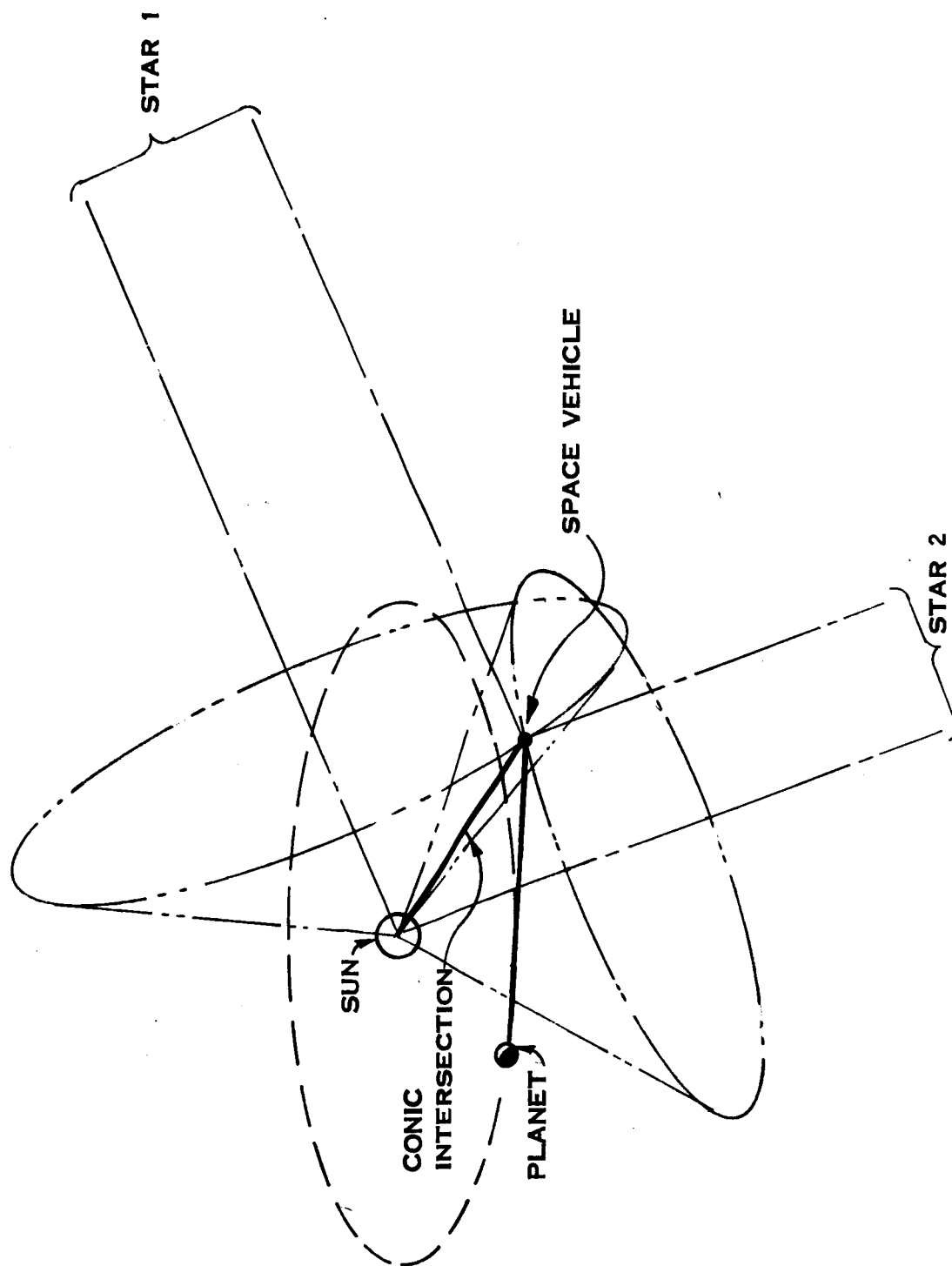
Figure 5-11. Solar-Position-Fix Geometry

The near-planet sightings probably will be performed in a region of approximately 1/2 to 10 million miles from the departure or arrival planet, as was shown in Figures 4-7a and 4-8a. This distance corresponds to a time period of approximately 1.5 to 20 days after departure or before arrival.

The zone in which the line-of-position measurements are performed is determined by the accuracy of the planet tracking. Figure 4-7a shows that, for the post-earth correction phase, there is no value in taking a planet sighting at too close a range; that is, at a departure time of 1.6 days from the earth and at a distance of 687,000 nm, the pheonomena-limited planet tracking accuracy is 20 arc seconds. As the distance from earth increases, the planet tracking error improves. At a departure distance of approximately 7,000,000 nm, the phenomena-limited planet tracking accuracy is 2 arc seconds. Considering the limitations of associated planet tracking instrumentation of roughly 2 arc seconds, there is no value in taking planet-star measurements past a range of 7 million miles.

When a sufficient set of planet-vehicles line-of-sight data has been obtained, this information, together with range data, may be used to determine the trajectory error relative to the nominal trajectory. This method assumes a variational guidance analysis technique.

5-11. Semiautomatic Post and Terminal Adjustment

Figure 5-12 shows the data acquisition and information flow for a generic semiautomatic post and terminal adjustment system. Data are acquired by use of a star tracker, a planet tracker, and a ranging stadimeter.

The star-tracker and planet-tracker measurements of the planet and nearby star provide two sets of two-axis gimbal angle data. These data are related to a common reference frame and therefore can be used to compute the planet-star angles. This comparison will permit a simple calculation of the attitude of the vehicle-planet line of sight.
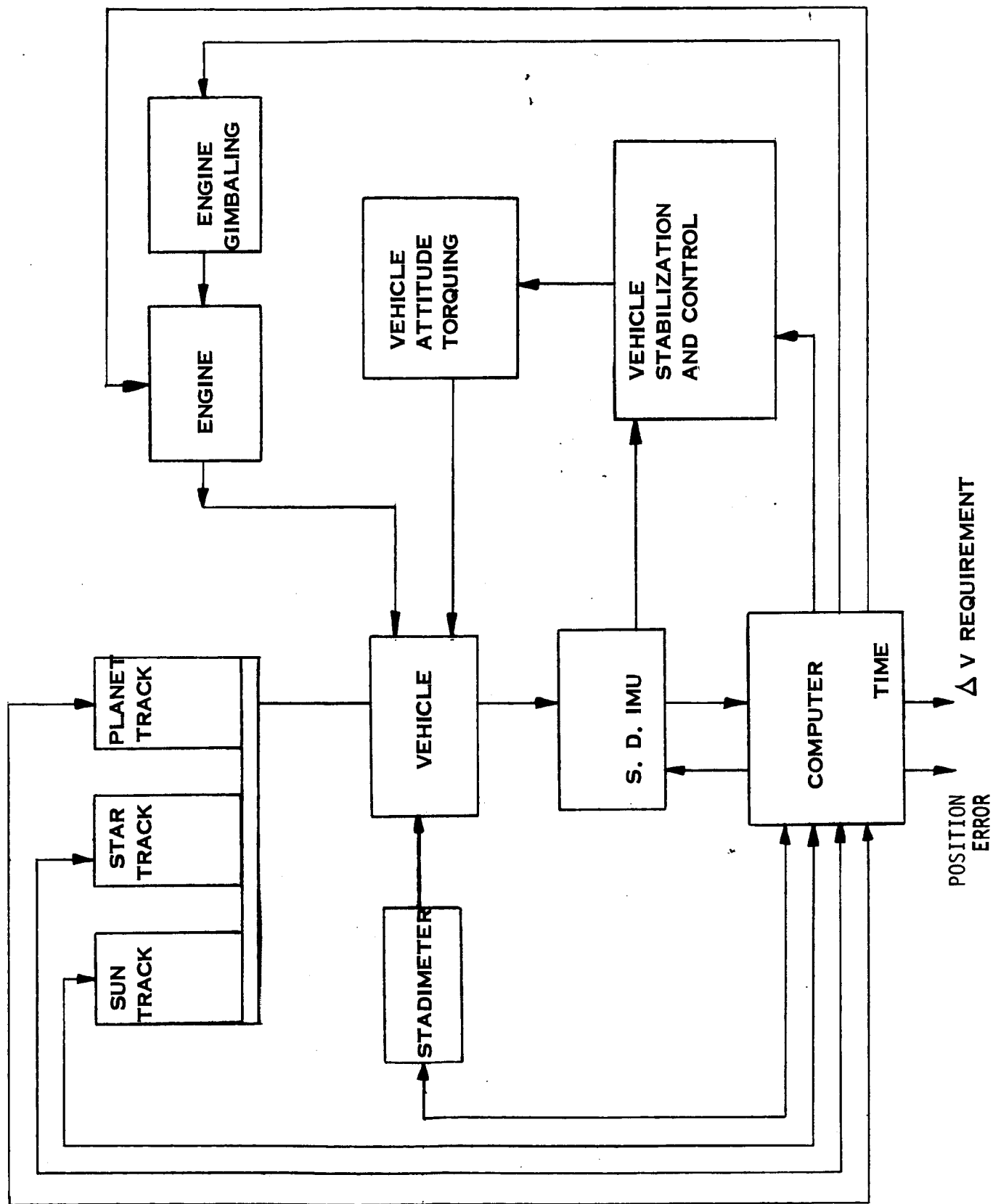
Figure 5-12. Semiautomatic Post and Terminal Adjustment

5-22

Vehicle-to-planet range information can be most accurately obtained from the injection trajectory computations. The stadimeter, however, can also be used to obtain range data. At departure and terminal adjustment ranges, the stadimeter is primarily making a planet-disc diameter measurement. Although a disc can be measured with extreme accuracy, the phenomenal limitations of measuring the angle subtended by the planet will result in large range errors. The addition of a sun tracker can supply sufficient data-acquisition capability to the star and planet trackers to allow for a solar-fix computation.

The sequence of principal operations for semiautomatic post and terminal adjustments is as follows:

1. Orient vehicle attitude to permit optical sensors to take position fix measurements.

2. Hold vehicle attitude stabilized by use of the SD IMU's gyros as part of a gimbaled servo loop. The loop consists of the SD IMU gyros, vehicle stabilization and control circuitry, and the vehicle attitude torquing hardware. Star-tracker data provide the inertial stabilization drift correction.

3. The computer commands optical track operations consisting of the sun track, two selected star tracks, and a planet and/or stadimeter track.

4. The computer computes vehicle position, vehicle-position error, and the requisite velocity increment for proper post or terminal course adjustment.

5. The computer commands the vehicle-attitude stabilization loop to the computed attitude for the course-correction engine firing.

6. The computer controls the engine firing time while the SD guidance and navigation system measures and controls the course-correction velocity impulse.

7. The navigation system commands engine cutoff when the desired course-correction velocity impulse has been achieved.

8. Repeat steps 1 through 4 at appropriate time intervals to check effect of course correction.

9. Compute impulse required for secondary course correction and compute desirability of initiating secondary course-correction impulse.

10. The semiautomatic instrumentation may also compute a trajectory correction by use of the planet-star comparison technique. For use of this technique, replace step 3 and 4 with step 3A and 4A.

3A. The computer commands optical track operations, consisting of a planet track, and track of adjacent elevation and azimuth stars.

4A. The computer computes the attitude of the planet-vehicle line, and the requisite velocity increment for proper post or terminal course adjustment.

5-12. *Aided-Manual Post and Terminal Adjustment*

Figure 5-13 shows the data acquisition and information flow for a generic aided-manual post and terminal adjustment system. The data acquisition may totally consist of planet-star comprisons if range data are obtained by dead reckoning; the planet-star comparator is an instrument which permits the direct measurement of the angle between a planet and an adjacent star or stars. Selection of the comparison stars in, and normal to, the orbit plane will simplify the calculation of departure or arrival trajectory line-of-position errors (Figure 5-10).

The planet-star comparison may be made by a number of different techniques, including a vidicon, space sextant, "optical-wedge" comparator, photographic techniques, and a simple optical-screen presentation with a grid background. Several illustrative techniques are described in Section 6.

The inherent capability of obtaining high precision in a small-angle measurement makes the planet-star comparison technique attractive. Small-angle techniques for measuring mechanical rotations have been implemented to precisions in excess of 0.1 arc second (Razdow Midarm); this capability is based on the ability to divide accurately a given angle by a factor. Due to the smaller division factor required for small-angle measurements, these measurements have generally been simpler and more precise.

The sequence of principal operations for aided-manual post and terminal adjustment is as follows:
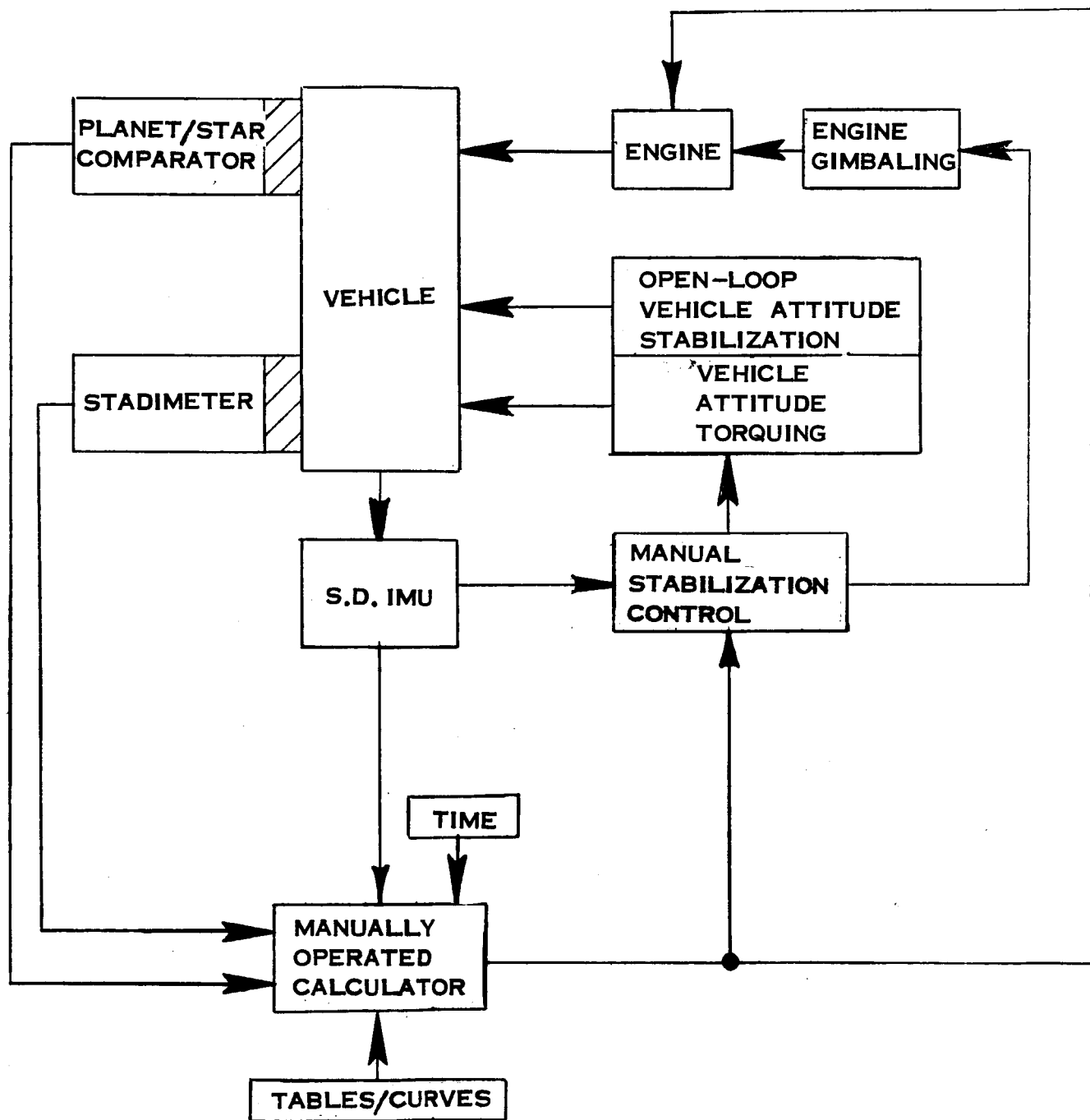
Figure 5-13. Aided-Manual Post and Terminal Adjustment

1. Manually control vehicle attitude torquing to place planet-star comparator in viewing position of the planet.

2. Maintain vehicle attitude by open-loop vehicle-attitude stabilization subsystem, and by intermittent manual vehicle attitude torque bias adjustments.

3. Crew members take a set of planet-star comparator measurements.

4. Calculate line-of-position and trajectory errors.

5. Compute post or terminal course adjustment ΔV.

6. Manually control vehicle attitude torquing to computed vehicle orientation for course correction engine firing.

7. Execute manual engine-ignition command executed.

8. Open-loop vehicle attitude stabilization coupled with manual control of vehicle attitude is utilized to maintain course-correction impulse attitude. The error signal for the manual attitude-control loop may be derived in a manner similar to that employed in the aided-manual injection stellar alignment.

9. Monitor in-line and normal velocity increments to minimize the normal component and to command engine cutoff when the computed course-correction ΔV has been attained. Manually controlled engine gimbaling and/or use of manually controlled multiple thrusters may be utilized in effecting the desired vehicle guidance.

10. Repeat steps 1 through 5 to determine whether or not any secondary course correction is required.

5-13. ORBIT ENTRY

Orbit entry may be attempted only after the terminal adjustments have accurately oriented the vehicle trajectory. With the predicted terminal trajectory established from the terminal-adjustment phase, orbit entry is essentially the reverse of the injection process described under heading 5-6.

Figures 5-7 and 4-10a are a three-dimensional and a plane view of the orbit-entry geometry, respectively. Orbit entry requires that the vehicle engine attitude be aligned with the computed ΔV attitude, and that the entry velocity impulse be applied at the proper range and/or range rate. Planetocentric position data may also be used to initiate the orbit-entry velocity impulse.

The vehicle engine attitude may be aligned to the proper orbit-entry attitude by use of a two-star reference. This reference can be used to generate an entry alignment error in a manner similar to the technique used to generate the injection alignment error (heading 5-6).

Range data may be readily supplied by an altimeter and/or a stadimeter.

Planetocentric position or latitude and longitude may be computed star-horizon measurements, as described ‥ under heading 5-1.

5-14. *Semiautomatic Orbit Entry*

Figure 5-14 shows the data acquisition and information flow for a semiautomatic orbit entry. The equipment utilized is the same as that required for a heliocentric injection.

The automatic horizon scanner and star tracker can provide sufficient data for a planetocentric position fix. This data, coupled with the altimeter for ranging and the set of star trackers for celestial attitude, provides complete sensory information for the initiation-orbit-entry guidance.

With the vehicle at the proper position and attitude, reverse thrust may be applied and the vehicle's automatic navigation-and-guidance system utilized to measure and control the precomputed orbit entry ΔV.

The two-axis star trackers track the celestial orbit entry attitude alignment stars to provide alignment-error data for the stabilization of the vehicle. The SD-IMU provides memory for the star-tracker alignment data.

The star trackers are also utilized with the horizon scanner to determine planetocentric position data. The utilization of the star trackers and horizon scanner is similar to that described under heading 5-1. The combination of planet range and range-rate data from the
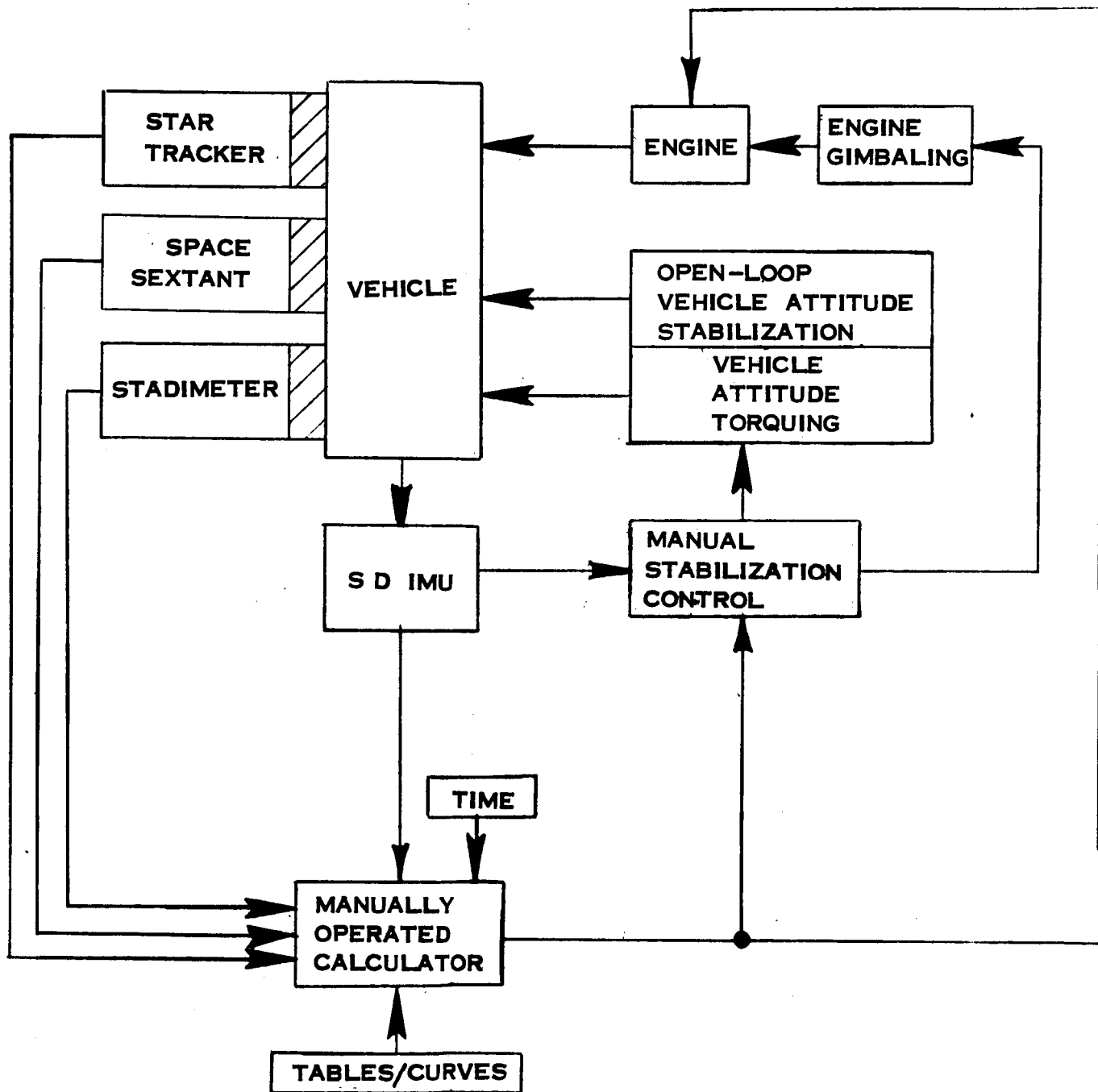
Figure 5-14. *Aided-Manual Approach for Cis-Martian Injection*

stadimeter provides an additional parameter of planetocentric information for the precise determination of engine ignition.

The sequence of principal operations for semiautomatic orbit entry is as follows:

1. The vehicle is stabilized in the precomputed attitude for proper orbit entry based on the terminal trajectory attitude calculations performed in the previous phase.

2. Vehicle attitude is held in stabilized mode by use of the SD IUM's attitude or rate reference, updated by the stellar alignment error display.

3. The computer commands operation of optical tracking, and navigation subsystems.

4. The optical-tracking operation consists of tracking the planet and an azimuth elevation star (equivalent to marine sextant measurement).

5. Altimeter subsystem activated to provide planet range and range-rate data.

6. The computer commands the automatic stabilization system to control the vehicle to the precomputed orbit-entry attitude.

7. Engine ignition is commanded when the measured range, range-rate and/or planetocentric position information are in agreement with the precomputed values for entry.

8. The vehicle's inertial guidance and navigation system is utilized to measure and control the orbit-entry impulse.

9. Engine cutoff is commanded when the strap-down navigation system has measured the requiste orbit-entry velocity impulse.

5-15. *Aided-Manual Orbit Entry*

Equipment for data acquisition and information flow for an aided-manual orbit-entry system are the same as those used for a heliocentric injection (Figure 5-4).

The space sextant and stadimeter supply the sensory data necessary for fixing planetocentric position. Vehicle attitude may be determined by taking a set of star sightings with the vehicle's inertial attitude-stabilization subsystem providing a short-term attitude memory.

The engine-burn portion of the orbit entry may utilize either an automatic or aided-manual mode of operation. As previously discussed in the section on injection, automatic operation is desired when high thrust levels are involved. This desirability, however, does not necessarily preclude the use of aided-manual guidance during the engine-burn portion of orbit entry.

The sequence of principal operations for aided-manual orbit entry is as follows:

1. The attitude of the vehicle is manually stabilized in the precomputed attitude for orbit entry.

2. Vehicle attitude held in desired preceding orientation (step 1) by star-sighting updating.

3. Crew members take sextant and stadimeter sightings.

4. Strapdown – IMU energized.

5. Engine ignition initiated at point where estimated planetocentric position and range match precomputed entry corridor.

6. Automatic inertial navigation-and-guidance system controls vehicle during engine burn.

7. Engine cutoff executed when the strap-down navigation system measures the requisite orbit-entry velocity impulse.

5-16. STATION KEEPING

The station-keeping phase contains the following navigation and guidance operations:

Orbit determination, correction, and maintenance;

Mapping;

Excursion-vehicle calculations for descent or landing and launch;

Rendezvous; and

Injection calculations for return trip.

The orbit determination is similar to the orbit-determination phase of Section 5-1, except for the time involved and number of orbit-determination iterations. The time period covered in the Earth-orbit determination should be less than 1 day, while the Martian-orbit determination phase will last approximately 50 days.

The mapping function covers a detailed mapping of the planet's surface to evaluate further preliminary site selections for the excursion vehicle and whatever mapping may be required for scientific information. To ensure a high-quality mapping of the planet's surface, a precision pointing subsystem may be required for the camera; this problem was investigated by Lozins (1964). The report indicated that camera pointing could be achieved to a high degree of precision (2 to 10 arc seconds).

One configuration that may be considered in the planet-mapping operation is to use a body-mounted camera instead of a gimbaled mounted camera. The high inertia provided by the body-coupled camera will provide superior pointing performance for a given pointing bandwidth and disturbance torque level.

Determining the excursion-vehicle landing and launch trajectories is primarily an energy management problem. Navigation and guidance of a vehicle from one point to another can be optimally defined by advanced control theory energy management techniques. For the case under study, the points are a function of time with a common planetocentric reference frame.

The energy management technique will define specific optimized point-to-point trajectories for descent and launch, depending on the criteria to be satisfied. For example, it will be necessary to consider such variables as vehicle stress, vehicle acceleration limits, skin temperature, and fuel consumption in selecting a descent trajectory. These computations are complex and may require an on-board computer if the entire process is performed in orbit. It is quite likely, however, that, given a preselected landing point and a nominal Mars orbit, much of the computation can be performed on the Earth prior to the mission. The on-board process would then be reduced to a much simplified variational technique based on tables, charts, nomographs, and the like to account for deviations from the nominal orbit. Control of the actual descent and launch operations involves the excursion vehilce with its specialized systems and will not be treated in this study.

Rendezvous after station keeping is similar to the Earth rendezvous problem and will not be discussed here. Rendezvous should not impose any special problems for the Mars orbital phase that are significantly different from the Earth-orbit rendezvous.

The navigation and guidance for injection into the Venus-Earth return trajectory is similar to the cis-Martian injection calculation. The Venus-Earth injection calculations will be performed and updated to provide detailed injection navigation and guidance requirements throughout the station-keeping period.

Section 6
Instrumentation

In this section, the characteristics of sensors required to produce navigation data are discussed in detail. This discussion provides basic information on sensors required for the consideration and study of alternative navigation-system configurations in Phases II and II.

The state of the art in navigation sensors is based largely on automatic approaches; this is reflected in the heavy emphasis on automation in the sensor systems described below. The mission under consideration, however, is manned, and the presence of a human crew provides an opportunity to use human skills and capabilities to reduce the complexity and enhance the reliability of essentially automatic sensor systems. In any of these activities, the crew can simplify equipment requirements by performing mode selection and sequencing, monitoring and acting as a link between systems.

It is meaningful to discuss these general crew functions in more detail only in the context of a specific configuration and this will be done during Phase II of the study. However, man can perform several functions with respect to specific sensor systems.

With respect to planet and sun trackers and horizon scanners, the crew can perform three functions which simplify navigation considerably: the crew can "fly" the vehicle to the correct altitude and then provide the necessary stabilization to keep the target bodies within the sensor field of view; the instrument operator can resolve the true null position, where there are secondary gradient null indications; and the operator can ensure that the instrument is operating and tracking properly.

With respect to star trackers, in addition to the functions described above, the operator can recognize patterns and identify stars; and, having brought the sensor to the correct orientation, he can ensure that the correct star is being tracked.

6-1. PLANET TRACKERS

The planet, or disk, tracker is related in function and mode of operation to the horizon scanner. The main difference is a somewhat artificial division based on the angular subtense of the planetary body. Horizon scanners may be thought of as those devices that work in the 20-to-180-degree angular subtend region, while planet trackers work at angles less than 20 degrees. The goal of either device is to find the direction to the geometric center of the planet.

Planet trackers can be separated into two general types. The first type depends on the planetary body radiating sufficient energy in the infrared region to make use of the total planet circumference, whether or not it is illuminated by sunlight. The second type depends on the sunlit crescent or gibbous phase. In either case, much of the recent work depends on the use of electronic image tubes. Using either the infrared image (full circumference) or visible-light image (crescent or gibbous phase), the positions of three points spaced along the outer circumference are sufficient to determine the center.

One lunar tracker, which uses visible light and mechanical edge scanning rather than complete imaging, is stated to have an accuracy of 20 seconds of arc. The instrument performs with a subtended lunar angle of between 0.5 and 9 degrees.

Another study on the use of electronic image tubes for planet tracking concluded that, with a 1000-line scan (regardless of tube type) and terrestial template matching on a monitor display, the center of Mars can be found within 8 arc seconds with Mars 2,000,000 miles distant. The angular subtense of the planet at this distance is 420 arc seconds. Similarly, it was concluded that the angular separation of the planet center and a nearby star could be determined to $\pm$0.029 degrees or $\pm$ 100 arc seconds.

Another method advocates a vehicle spinning with a known rotational velocity about an axis normal to the ecliptic plane with a rigidly mounted electro-optical telescope aboard. The telescope is made up of a lens, a focal plane containing slits parallel to the axis of rotation, and a photomultiplier that responds to the visible light signals passing through the slits. As the vehicle rotates, a time sequence of varying length pulses is obtained. The pulse is defined by the location of the celestial body along the azimuth and elevation directions, the angular subtense of the body, its state of terminator or edge definition, and the bias and spectral cutoff level of the photomultiplier. In a cislunar mission, the accuracy of finding a star position or the lunar center is quoted to be slightly greater than 5 seconds of arc, the larger part of the error being instrumental.

In a June 1966 study report on the Voyager mission, General Electric proposed the use of a single image tube, possibly the ABC image orthicon developed by General Electric. The television system will continually transmit a mosaic containing images of Canopus, the Sun, and Mars. Accuracy of navigational measurement is based on the least television line readout position on the tube. The error is expected to be in the region of 0.1 milliradian (20 arc seconds).

All planet trackers that employ television or related pickup tubes are limited by the least-resolution interval, usually one or several television lines, and the dynamic range limitation. Nevertheless, television image methods have many advantages. These are the possibilities for earth-bound readout, wide-field recording which might include the planet and several surrounding stars, and high sensitivity in any one of several spectral regions.

6-2. HORIZON SCANNERS

Horizon scanners are automatic tracking devices which operate as multiple elements of a larger system to provide data for the system that is used to obtain the direction to the center of a planetary body.

As an instrument class, horizon scanners usually include only those infrared devices used for maintaining the local vertical direction for orbiting satellites. The orbital mission precludes the use of any optical device which operates only in the visible region, because the vehicle passes periodically over completely dark regions. By necessity, the celestial body for which local vertical is being determined must have certain characteristics to ensure success: it must be warm enough that a detectable thermal discontinuity exists at the horizon; the discontinuity or gradient should be sharp; and the radiance should be reasonably uniform over the planet surface.

The accuracy with which the horizon can be determined depends on the steepness of the horizon gradient, which, in turn, is dependent on the atmospheric characteristics. The moon exhibits an infinite gradient, although extreme terrain discontinuities near the horizon detract from the otherwise ideal horizon signal. The earth has its well-known atmospheric windows, but the signal also suffers degradations because of low energy or a very gradual gradient in the window regions. Less information is available on the horizon gradients of Mars and Venus. There are indications that the atmosphere of Mars is very tenuous and will therefore not diffuse the horizon significantly. Venus has a very dense atmosphere of unknown depth, but exhibits a well-defined top of the cloud deck. Consequently, fewer difficulties are to be expected in the horizon sensing for Mars and Venus than for the Earth or Moon.

Because planetary temperatures vary from 120 to 380° K, the thermal detectors used must respond in the region of 8 to 40 microns. The use of the more sensitive photoconductors, such as zinc or copper-doped germanium, are not feasible for long space missions because of the requirement for maintaining the detectors at liquid-helium temperatures. Only thermal detectors, such as thermistor and metal bolometers and thermocouples, are suitable.

Horizon scanners can be grouped into three general categories:

    1. Conical scan,

    2. Edge tracking, and

3. Radiometric balance.

In the conical scan, a relatively small detector field is made to scan along the periphery of a large hollow cone; the mechanism of the scan is supplied by mechanically rotating optical prisms or mirrors. The cone may have an apex angle as large as 180 degrees, although 30 to 120 degrees is more common. Two such scanners with orthogonal or parallel scan axes provide two sets of pulses which are related to the dwell time of the detector field within the planet envelope. An analysis of the relative lengths of the two pulses, and the positions of the pulse leading and tracking edges within the scan cycle, provide for measurement of the pitch and roll attitude angles of the vehicle. The The mean length of the pulses can also be used to measure range or altitude.

Edge tracking provides more accuracy than the conical scan. An array of detectors, each with an optical dithering means, is pointed (with the aid of an auxiliary coarse pointing device) such that the direction of each member of the array can be oscillated locally across the edge of the planet. The arrayed elements are spaced evenly about the circumference of the body. Fine pointing involves the adjustment of the entire detector group direction such that the output signals from all detectors are the same.

The radiometric balance technique, which does not involve any scanning or moving parts, is the simplest of the three methods. In effect, the planet disk is imaged onto four detectors in quadrature. Comparison of the four signal levels indicates the direction of imbalance. Proper pointing of the detector with reference to the basic coordinate system provides the directional angles to the planet center.

The major limitations on the three methods are related to the chief data for the respective modes of operation. In the conical horizon scanner, it is the time definition of the planet pulse edges; in the edge tracker, it is also the definition of the pulse edges, but in addition there is a limitation due to the resolver readout accuracy; the limitations on the radiometric balance sensor are due to false

additive signals in each quadrant, such as unequal planetary temperatures, drift in the thermopile combination, or the sun in a portion of one quadrant. Table 6-1 defines accuracies of several horizon-scanner types for different planetary bodies.

6-3. SUN TRACKERS

Sun trackers, as self-contained, automatic devices for obtaining the line of sight to the sun, usually differ in their mode of operation from other trackers because of the vast difference in the target object itself. Because of the high solar irradiance supplied at the sensor, the solar disk need not be imaged in the usual sense. The simplest sun tracker, for instance, is a photocell whose output is proportional to the cosine of the angle of incidence of the sun's rays; these devices, manufactured by Ball Brothers Co., Inc., have demonstrated accuracies of 2 to 3 degrees. Limitation on the accuracy is that due to slowly varying cosine curve in the null region.

Other gated sensors indicate when the solar line of sight is in a selected direction. This is done, in effect, by allowing the sunlight to pass through a slit to a masked detector, where the masking config- uration is related to the desired line of sight. Accuracy is stated by Adcole Corporation to vary from 0.25 to 5 degrees, depending on the total acquisition field of view.

Further refinements in the above Adcole Corporation approach have led to solar trackers with a digital readout of the solar angle. This is done by using digitally coded masking at the "focal plane" of this slit. The output is an absolute readout of the solar angle which is limited by the least significant bit in the encoded mask. Models are available which read to 1 and 0.5 degrees. One such device is capable of single- axis readout only. Because of its simplicity, complete two-axis read- out is obtained by using two similar elements with orthogonal slits. Readout again is absolute, the least reading for each axis being 1 or 0.5 degrees.

Table 6-1. Summary of Horizon Sensor Accuracies

Horizon Sensor Type	Range of Accuracies Against Venus (degrees)	Range of Accuracies Against Earth (degrees)	Range of Accuracies Against Mars in First or Last Quarter Phase (degrees)	Range of Accuracies Against Moon in First or Last Quarter Phase (degrees)
Conical scan sensors				
a. Simple conical scanner	±0.1 to ±0.3	±0.2 to ±0.3	±0.3 to ±1	Requires elimination of trailing-edge error.
b. "Space-scan" conical scanner	±0.05 to ±0.1	$<\pm0.1$	±0.1 to ±0.3	$<\pm0.3$
Edge tracker	±0.05 to ±0.1	±0.1 to ±0.3 (Atmospheric CO_2 band used)	Requires means for discrimination of true horizon edge from cloud edges.	Requires means for discrimination of true horizon edge from crater edge.
Radiometric balance sensor	±0.5 to $+2$	±0.5 to ±2	$+3$ to ±10	Not applicable except for very coarse pointing.

Although the least significant bit of the encoded mask defines the resolution of the output, resolution is also limited by the subtense of the solar disk at the point of measurement. If the solar direction is to be measured in the vicinity of the earth with one of these slit trackers, the slit must pass a 0.5 degree unfocused beam, which results in a resolution of about that magnitude in the readout.

The accuracy of the basic Adcole digital-slit and encoded-mask approach can be enhanced by using phase information in the output signal. The position of half the encoded mask of a typical one-axis tracker is changed such that the output signals from each half are in quadrature. The resultant phase of the signal can then be determined and an order of magnitude gained in accuracy. Solar angles have been measured to $\pm$ 0.06 degree.

Ball Brothers have also accomplished accuracies of $\pm$ 0.1 degree by using shaded mosaic arrays of solar "eyes".

Solar tracking capability at this time is of the 0.05 - to 0.1-degree order of accuracy, which is similar to that of other disk-tracker types. It is expected that at least an order of magnitude gain can be made by improving the electronic circuitry and by using imagining techniques and manual aid.

6-4. STAR TRACKERS

Star trackers are electro-optical instruments used in spacecraft to provide navigational and stabilization information. The information provided is the deviation between a predetermined line of sight and the actual line of sight formed by the spacecraft, the tracking star, and other reference targets. This information is in the form of an electrical signal which, upon exceeding a selected deviation, pulses small, cold-gas nozzles.

Star trackers utilize an objective mirror which collects and images to a point the impinging star irradiance. A modulator scans the image and encodes it into a usable form from which angular deviation

can be reduced. A radiation-sensitive detector then accepts the encoded information and transduces it into a usable electrical signal.

Photomultiplier tubes and image-dissector tubes are commonly used as the photodetector. If a photomultiplier tube is used, a mechanical modulator must be utilized. This is a scanning device usually utilizing either a spinning reticle or a vibrating slit with an assemblage of gears, cams, and other moving parts. When an image-dissector tube is used, modulation is accomplished using the small, electrostatically focused beam which, as part of the image dissector tube, electronically scans the photo-surface.

System characteristics for star trackers are usually described in terms of initial acquisition capability, detectable star magnitude, and output accuracies. Other important characteristics are size, weight, life, power consumption, and ruggedness.

The characteristics for several typical star trackers are listed in Table 6-2. The status of these trackers is either "flown" or "flight prototype". In general, the accuracies of the flown trackers are more realistic than the prototypes. The accuracies are mostly limited by the inherent noise of the photodetector and the limitations of the tracker field of view.

For a representative tracker, in which the photodetector is a photomultiplier tube, dark-current noise is 3.08608×10^{-9} amps. When a star is tracked, a change in signal current is produced as the star image is linearly displaced along an axis defined on the photocathode. When the ratio of signal current to dark current is one, the star image is displaced 0.0001288 inch, which is then the displacement error caused by noise. The angular error, which is the output error, is arrived at by dividing the displacement by the focal length of the collecting optics. For this example, the output error is 3.8 arc seconds.

The output error can be decreased by increasing the focal length. This change, however, is limited by the field-of-view requirements, since the field of view decreases as the focal length is increased. An

Table 6-2. Summary of Star-Tracker Characteristics

Identity	Manufacturer*	Scanned Field of View	Accuracy	Axes	Sensitivity (Star Magnitude)	Detector†	Size (inches)	Weight (lbs)	Power (watts)	Life	Status (12/31/65)
OAO Startracker	Kollsman	1° x 1°	30"	2	+2	PM	11 x 17 x 16 + 11 x 16 x 4	23.6 + 18.5	17.5 + 10.0	1-yr mission	Flown
Canopus Tracker	Barnes Eng. Co. (JPL)	5° x 11°	0.1° null	1	+2.3	ID	4 x 5 x 11	5	1.5	2.0 x 10^5 hr	Flown
Dual Mode Startracker	ITT	8° x 8° or 32'x32'	5" rms	2	+3	ID	5 x 10-1/2 x 5	9.5	8.0	-	Prototype
Sun/Star Sensor	Nortronics	30'	10"	2	+3	PM	105 cu in.	9	8.0	-	Prototype
Canopus Tracker	Santa Barbara Research Ctr.	+2° x 5°	0.1°	1	can. +0.5	PM	-	4.9	-	2-week mission	Flown
NCN 121 Startracker	Nortronics	10 min.x 10 min.	2.8" x 1.0"	2	+3.5	VID	265 cu in.	9.5	12	1.8 x 10^3 hr	Prototype
OAO Back-up Startracker	Bendix Corp. (ITT)	1° x 1°	9"	2	+2.5	ID	5-5/8 x 5-1/4 x 5-1/4	6	4.5	1-yr mission	Prototype

*JPL = Jet Propulsion Laboratories

ITT = International Telephone and Telegraph Corporation - Federal Laboratories

† PM = Photomultiplier tube

ID = Image dissector tube

VID = Vidicon tube

increased focal length will also result in a larger package. For example, a tracker with an accuracy of 10 seconds and field of view of 30 minutes can be housed in a 105-cubic-inch package, whereas a tracker with accuracy of 2.8 seconds and field of view of 10 minutes require a package of 265 cubic inches.

Field of view also is important in the initial-acquisition capability and the tracking-star selection. The initial acquisition is complicated when stars of similar magnitude are in the field of view. A tracking star with magnitude bright enough to be distinct in a limited field of view is desired. In a 1-degree field of view, one star is brighter in the field when a +8-magnitude star is chosen; this is large when compared to the 0.013 stars in the 1-degree field when a +4-magnitude star is chosen, or the 0.0014 stars in the field when a +3-magnitude star is chosen.

The tracking star, however, can be disqualified on the basis of signal level. The just-detectable star magnitude is a function of the sky background, the photodetector noise, and the aperture size of the collecting objective. If the sky background and photodetector noise are fixed, then for a particular star magnitude there is a unique aperture size which yields a photodetection signal-to-noise ratio of one. Taking sky background to be 1.2×10^{-15} watts/cm^{2}degree^2 (background outside the atmosphere), and considering the noise of the 1P21 photomultiplier tube, the aperture required to just detect a +2.5-magnitude star is 0.45 cm^2. When tracking a +5.0-magnitude star, the aperture required is 4.5 cm^2.

Increasing the aperture area to 78 cm^2 (10 cm diameter), the signal-to-noise ratio for a +2.5-magnitude star is approximately 150. As shown in Table 6-2, sensitivities (in star-magnitude units) range between +2.0 and +3.5. This is indicative of the good acquisition capability and the workable signal-to-noise ratios afforded by this magnitude range.

6-5. RADAR ALTIMETERS

An accurate measurement of altitude is required for controlling the parking orbit. Parking orbits are needed leaving the earth and also before landing on Mars. A nominal parking orbit may be considered to be at 500 nautical miles (approximately 1000 km) above the surface of either planet. To adjust the flight velocities effectively, it is desirable to measure the orbital altitude to a 1-percent accuracy.

Present-day radar altimeters have been designed to operate from aircraft altitude ranges to ground level with the extreme accuracy desired near ground level. However, it is perfectly feasible by state-of-the-art techniques to design a satellite radar altimeter of the desired accuracy and range.

Radar altimeters are designed on the basis of measurement of the pulse echo delay in a pulsed-radar system, or measurement of frequency shift in a frequency-modulated, continuous-wave (FM-CW) radar system. The choice of system depends on the size and weight *versus* complexity tradeoff. Pulsed radars may be larger and heavier due to the peak powers required, but they are less complex; FM-CW radars are smaller and lighter, but more complex. The complexity factor affects reliability, so that consideration is usually given to both designs when design tradeoffs are made.

To obtain some insight into the complexity factor and size and weight factors, it is instructive to evaluate typical designs. For a bandwidth-limited, pulsed radar, the 3σ accuracy can be determined from the following relation:

$$\text{Range accuracy } (3\sigma) = \frac{c}{4BR \sqrt{S/N}}$$

where c is the speed of light, B is the power bandwidth, R is the range, and S/N is the signal power to noise power ratio. At a 1000-km range, a 20-db signal-to-noise ratio and an accuracy of 1 percent, the 3-db bandwidth is 1200 cycles per second.

The equivalent equation for the FM-CW radar is

$$\text{Range accuracy } (3\sigma) = \frac{c}{4R\Delta f}$$

where Δf is the frequency shift. For the same conditions, the frequency shift is 7500 cycles per second; thus, the FM-CW radar requires a much wider band system. HOwever, the average transmitter power required can be approximately the same for either system with the pulsed radar peak power being may times higher. It is estimated that approximately 10 watts average power would be required, provided that a low-noise-figure, high-sensitivity superheterodyne receiver is considered. Present FM-CW crystal-video radar altimeters operate at C-band with an average power of 1.5 watts at an altitude of 20,000 feet, with an antenna beamwidth of 60 degrees. Thus, with a superheterodyne and an antenna beamwidth of 2 degrees, the power required is only an order of magnitude higher, even though the range is between two and three orders of magnitude greater, and power increases as the fourth power of range.

If radar altimetry is employed beyond the 500-nm orbital range, its utility is limited by rapidly increasing required power, and by antenna-pointing accuracy. Therefore, at large range values, it is undesirable to depend on radar altimeters, since at these distances planet subtending systems are more effective.

6-6. MANUALLY OPERATED SENSORS

A series of navigation experiments carried out on the Gemini 4 and 7 flights (Jorris and Silva, 1966) have demonstrated man's ability to obtain accurate navigation data in space by means of a manually operated space sextant. The sextant is used for the same type of angular measurement provided by the automatic trackers described above. A second manual instrument, the stadimeter, can be used to obtain range information. Such instruments take maximum advantage of man's ability to recognize star patterns, and to identify individual stars. Perhaps the most important human skill which makes a manually operated sextant attractive when compared with an automatic system is the ability of a man, given

the proper visual information, to locate the center of a planet disk. Man is capable of compensating for gibbous effects, ellipticity, and terrain irregularities, which are the limiting phenomenal factors in automatic planet trackers.

6-7. *Sextants*

All sextants operate on the principle illustrated in Figure 6-1. An undeviated line of sight to a reference feature, such as a planet marking, planet limb, or a star, is maintained by manual, gimbaled, or vehicle thrust correction. A second line of sight to another object, usually a star, is made through an adjustable mirror which is used to superimpose the second object image on the first. The amount of adjustment that is applied to the rotating mirror is a measure of the angular subtense between the two objects.

The ability to measure the angle between the two objects depends on several effects which have been evaluated on space simulators and the actual manned Gemini flights GT-4 and GT-7*:

1. *Star-star measurements give the greatest accuracy.* 20-arc-second accuracy was obtained using a hand-held sextant having a 4.5 power telescope, a 15-degree field of view, and a resolution of 3.6 arc seconds. Another experiment with the same type of sextant showed standard deviations of 10.5 arc seconds around a mean error of 7.5 seconds for the star-star, and 16.5 arc seconds about a mean of 20.5 seconds for a star-near planet limb measurement.

2. *Increasing the magnifying power of the telescope improves the accuracy.* The results of a simulated Apollo midcourse navigation problem has demonstrated errors having standard deviations of 1.5 to 3.0 arc seconds with mean errors of 3.0 and 6.0 seconds. The telescope powers were 28x and 40x as compared with 4.5x for the Gemini mission described above. The errors were also consistently smaller by 1 or 2 arc seconds with the 40x setting.

---

*Acken, R.A., 1966
Duke and Jones, 1964
Jorris and Silva, 1966
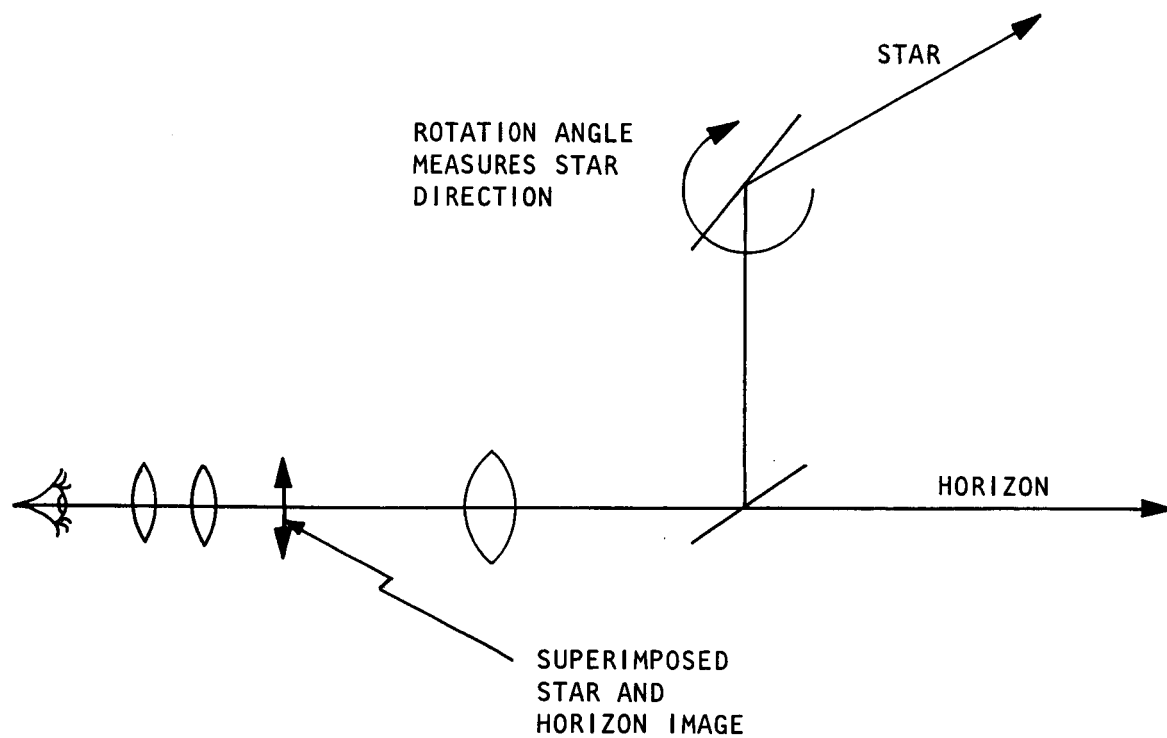Lampkin and Randle, 1965
White, U.C., 1966

Figure 6-1. Celestial Sextant

3. *Measurement between two objects of more nearly equally brightness improved accuracy.*

4. *Gimbaled sextant readings invariably show better results than hand-held readings.* However, the difference is not as great as one would suspect. For instance, with star-star readings, the hand-held sextant had a standard deviation of 10.5 seconds about a mean of 7.5 seconds, while the gimbaled sextant gave a standard deviation of 6.0 seconds about a mean of 5.0 seconds.

5. *Measurements made with simulated constant or sinusoidal vehicle angular rates showed higher repeatability than that for the random vehicle motions.*

6. *Performance varies greatly with operators.* In one experiment, the individual standard deviations varied from 10 to 100 arc seconds.

The results of these experiments indicate that man can use a space sextant to good advantage in an interplanetary mission. The sextant chosen for the job should have reasonably high magnifying power, possibly in the 6x to 50x range. It is desirable to mount the sextant in gimbals and possibly use remote control; however, satisfactory accuracy levels may be achieved with a properly designed hand-held instrument.

6-8. *Planet-Star Comparator*

The use of man as a functioning element in the navigation system permits consideration of a great variety of nonconventional instruments. Man has the ability, for instance, to recognize a particular star pattern at a glance. He can determine with some precision the position of the geometrical center of a planet in its crescent or gibbous phase. The same ability is evident in bringing a star image to the planet horizon, much as in terrestrial sextant fixes. He can detect quite accurately the very slight wobble of minutely decentered objects in a rotating field of view. All of these capabilities would require unusual complexity in instrumentation designed for the same task.

An example of the type of manual device that could be used for measuring the angle between a star and a planet center or edge is illustrated in Figure 6-2. This device, which may be regarded as an ultrasophisticated sextant, utilizes the convenience of a narrow field of view both for improved accuracy and practicality for observation through a narrow spacecraft window. Figure 6-2 shows an imaging objective lens in front of which a beamsplitter superposes two lines of sight. One line of sight passes straight through the beamsplitter toward the planet. The upper line of sight is directed by a Risley prism. By proper adjustment of the optical wedges about the optical axis, the star image can be made to appear at the center or edge of the planet image as shown. A readout of the two wedge angles will then furnish both the azimuth angle of the star relative to any assigned direction on the face of the planet image, and the total angle between the star and planet center or edge. The duplication of the star line-of-sight deviator indicates that two or more stars can be included simultaneously in the celestial fix.

It   been mentioned that the human operator is very sensitive to the wobbling motion associated with a slightly decentered rotating object. The effect has been used, for instance, in truing up work in a lathe or in centering and edging optical elements. Provision can also be made in this device for such capability. A Dove prism is shown immediately in front of the objective lens. It is intended that the man rotate the prism manually or with a variable-speed motor, as needed, to rotate the field of view. With the Dove prism at the position shown, all objects in the field of view will rotate together. If either the stars or planet are slightly off-center, the wobble will be quite noticeable and corrective measures can be taken.

The planet image in its gibbous or crescent phase will exhibit wobble or flickering under all conditions. Rather than eliminate wobble, the object of the rotation is to adjust the telescope line of sight to the planet such that the *smallest diameter* blurred disk is seen. The planet is then rotating about its geometric center and its circumference will exhibit a very sharp unwavering outline against black space.
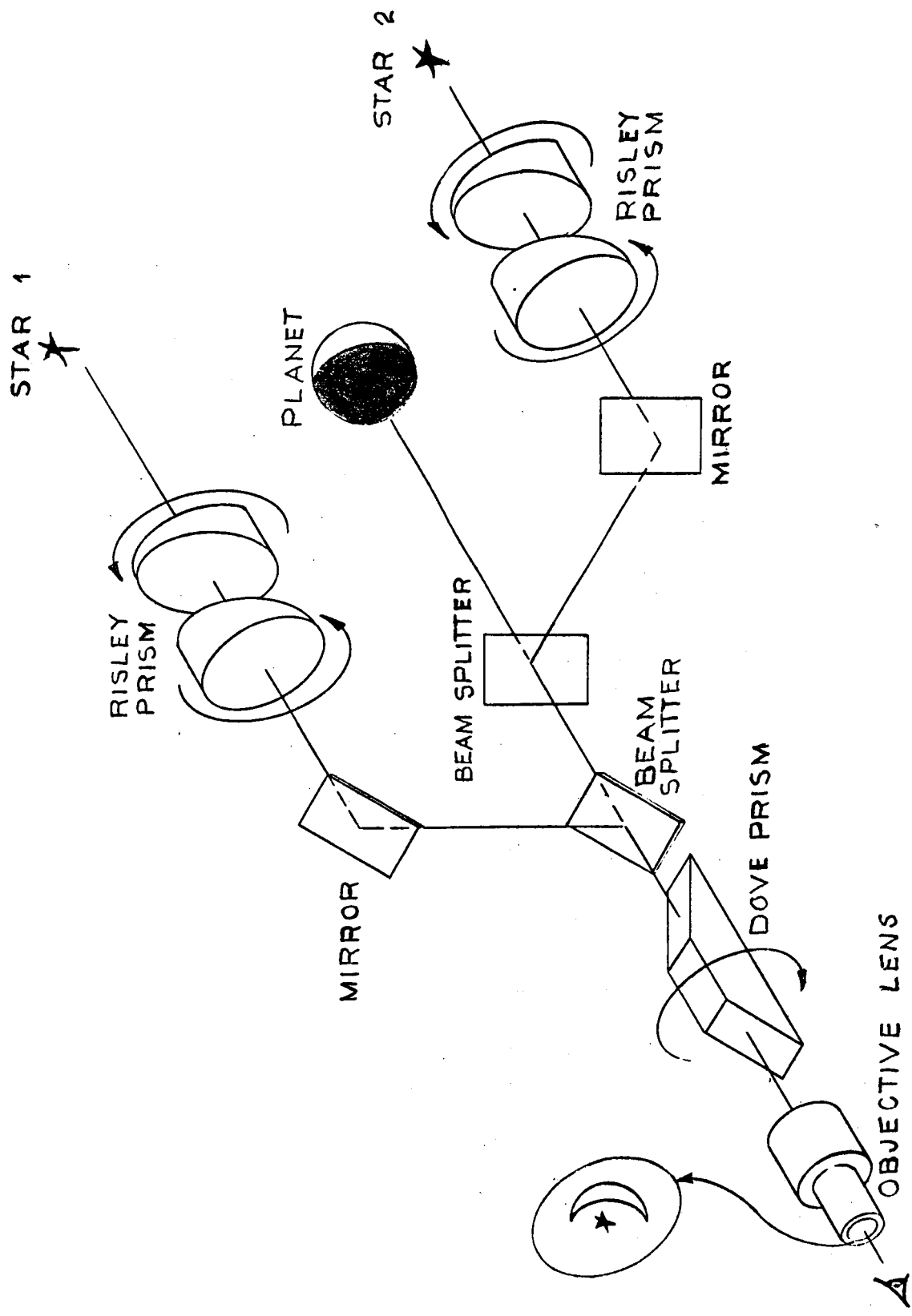
6-17

Figure 6-2. Planet-Star Comparator

Although man's capabilities for such activities as locating the center of a circle, wobble detection, constructing right angles unassisted, and so forth, have not been studied extensively, estimates can be made of his accuracy. An experiment with a hand-held space sextant has demonstrated an accuracy of 18 arc seconds. The truing up of a lens element in a centering and edging machine by unassisted observation of the wobbling of a reflected light image at the lens surface can be shown to be accurate to several seconds. A very sensitive test for the accuracy of the 90-degree roof angle on Amici prisms is to study the reflected image of the observer's own pupil, where a very few arc seconds of error results in a cat's eye or a doubled pupil appearance, depending on the direction of the error.

6-9. *Stadimeter*

The hand-held stadimeter optically determines range from a spacecraft to Earth, Moon, or other neighboring planetary bodies. The instrument determines range as a function of the measured curvature of the portion of horizon viewed through a sight-angle-limited flat viewing window of the spacecraft. By optically measuring the angle between two chords through three equidistantly spaced points on the horizon, the stadimeter determines the curvature of a limited region of the viewed horizon.

Three 14-degree portions of the horizon are viewed. These portions, separated by 45 degrees, and centered around the intersection of the chords with the horizon, are superimposed utilizing a pair of special deviation prisms. Rotation of one prism relative to the other results in the intersection of the three horizon sections. The rotational angle is related to the orbital altitude through a mathematical relationship or auxillary graphs. The general characteristics of a stadimeter manufactured by Kollsman Instrument Co. for the Air Force are listed in Table 6-3.

Table 6-3. General Characteristics of a Stadimeter

Characteristics	1-Inch Focal-Length Eyepiece	2-Inch Focal-Length Eyepiece
Size (L x W x H) in inches	$6\frac{57}{54} \times 6\frac{7}{32} \times 5\frac{17}{32}$	$7\frac{17}{64} \times 6\frac{7}{32} \times 5\frac{17}{32}$
Weight	8 lb, 3 oz	8 lb, 8 oz
Magnification	4.5X	2.25X
Field of view (degrees)	14	14
Exit pupil (mm)	7	14
Eye relief (mm)	19	74
Diopter adjustment	-3 to +4	-2 to +2
Resolution (seconds)	10	10
Image	Erect	Erect
Range (degrees)	-1 to 21	-1 to 21

6-10. *Photographic Approaches*

An alternative to real-time optical measurements can be provided by a photographic system. The advantages of such a system are that stabilization requirements are far less stringent; measurements are made more carefully; background stars provide for self-calibration of each photograph; and, given batch-processing of photographs, a series of navigational sightings can be made in less time than would be required for an equal number of direct sightings.

Havill (1963) describes a photographic technique to provide navigation data for midcourse corrections. While Havill's technique is designed to obtain distances and line-of-sight angles to the Earth from a Moon-Earth trajectory, the measurement techniques are generally applicable to near-body navigation procedures.

Havill's technique involves taking a series of photographs of a near celestial body with two stars of known angular separation in the background. Using the stars for calibrations, the distance to the body is obtained by measuring the diameter of the image. The line-of-sight angle traversed in successive images is obtained by superimposing the background stars and measuring the center-to-center distance between two successive images. In Havill's study, the near body was the Earth; given the time between successive images, the angular separation of the background stars on the celestial sphere, and the diameter of the Earth, the trajectory parameters can be computed.

To evaluate the accuracy limitations of this procedure, a series of tests was conducted in which subjects performed the measurements on photographic images of disks tilted so as to correspond to the Earth's ellipticity as seen from various points in space.

Two devices provided accurate measurement of the photographic images: a transparent overlay with accurately inscribed circles, and a small 30-power shop microscope. The inscribed circles on the transparent overlay were drawn with a radial separation of 0.1 inch and a line weight of about 0.002 inch. The smallest division of the shop microscope was 0.001 inch, and it could be read to about half this distance. A 1/32-inch hole was drilled at the common center of the circles inscribed on the overlay and a sharp tool which fit tightly into this hole marked the photographic image at its center.

The maximum error in measurement of disk diameter was 0.0029 inch or 0.035 percent of the disk's diameter. Maximum center-to-center error was 0.25 percent of the diameter; at the ranges simulated in the study, these figures correspond to angular errors of about 2 and 7 arc seconds, respectively. The time required to perform each measurement was about 10 minutes, and the time to perform the required calculations to obtain orbital elements was about 15 minutes.

Havill concludes that the technique studied could provide a basis for an adequate navigation system. He points out that a system of tables and nomographs could be employed to reduce the number of calculations required.

6-11. ATTITUDE CONTROL

Attitude control must be exercised at two points in a navigation-and-guidance sequence: (1) to permit navigational observations to be made, the vehicle must be brought to and stabilized at an attitude which maintains the target objects within the sensor field of view; and (2) for thrusting, the vehicle must be brought to and stabilized at some precomputed attitude to ensure the correct thrust angle throughout the thrust period. The required attitude control may be accomplished by the crew in several ways.

If an IMU is available, the pilot can simply "dial" the desired attitudes into the IMU in terms of the inertial coordinates. The IMU would then simply slew the vehicle to that attitude and provide the necessary stabilization.

However, given the presence of a human pilot, the attitude-control system can be simplified by having the pilot fly the craft to the appropriate attitude. This can be accomplished by providing the pilot with an optical display of the necessary visual information. Pointing data for thrusting or observation would be given in the form of two angles along and normal to the line between two reference stars. An example of how such an instrument might work is as follows.

The geometrical information required to fix the point could be fed into the display by having the pilot maneuver the spacecraft so as to place both reference stars on a horizonal crosshair, with one star at the center of the reticule. Dialing in the two angles, horizontal with respect of the star in the center, and normal to the horizonal line would geometrically fix the thrust orientation point on the display, and would optically drive one of the two reference stars to that point. The pilot's task would then be to maneuver and maintain the reference star in the center of the display by means of a crosshair sight. Given a very low gain mode in the manual attitude control system, a human pilot could provide the alignment with a very high degree of accuracy, eliminating the need for a star tracker. At this point, having accurately

aligned the vehicle, the pilot could select an automatic stabilization mode to maintain the correct attitude during the thrust period.

Alternatively, stabilization during thrust could be provided by the pilot by controlling attitude directly with reference to the display described above. For small, low-thrust corrections, this seems feasible. However, large thrust corrections are likely to produce attitude rates and noise of a magnitude and frequency beyond the ability of a human operator to control.

6-12. VELOCITY-INCREMENT MEASUREMENT

In the execution of necessary enroute trajectory corrections, some incremental velocity is generally applied to spacecraft. The measurement philosophy associated with this correction can be of the open-loop tracking type, or, in various degrees of complexity, a true on-board measuring system. If the thrust source is of a very low value, the trend would be toward an open-loop system, in which the correction is made by controling the engine on time; the effect is then determined by using the basic navigation system to redetermine the new trajectory. With higher thrust levels, however, a direct velocity-increment measurement would be required.

An inertial measurement unit capable of providing the needed instrumentation could be employed in either a gimbaled or strap-down configuration. If a strap-down angular measurement system were used for attitude stabilization, the same gyros could be used as a measurement system with the addition of an accelerometer triad. Three accelerometers mounted to the same substructure as the gyros with parallel aligned input axes result in a simple configuration. When this approach is used, the ΔV thrust is converted into a stabilized computational reference frame. The reference frame is computed from the base rotation data as measured by the gyros. The accelerometer data are then rotated into the stabilized computation frame, so that velocity increments can be computed in a fixed inertial reference frame.

Because strap-down inertial navigation techniques are mechanically simple, good reliability may be expected over the comparatively long Mars mission time. To improve reliability, a grouping of six SD IMUs, together with appropriate spares, could be considered.

A gimbaled IMU might be considered as a means of supplying vehicle-attitude data and velocity-increment measurements. The gimbaled IMU differs primarily from the strap-down unit in that the accelerometers are maintained in a physical inertial-measurement frame by a set of three or four gimbals and associated torquers. Although this configuration provides better inertial reference drift performance, because the gyros operate at a null, the gimbaling mechanization and readout equipment are mechanically complex. Reliability estimates indicate strap-down performance may be thousands of hours, while gimbaled performance is limited to hundreds of hours.

REFERENCES

Acken, R. A., "Navigator Performance Studies for Space Navigation Using the NASA CU-990 Aircraft", presented at the Manual/Autonomous Space Navigation Symposium of the AAS, Valley Forge, Pa., October 1966.

Battin, R. H., *Astronautical Guidance*, McGraw-Hill, 1964.

Bowditch, Nathaniel, *The New American Practical Navigator: being an epitome of navigation; containing all the tables necessary to be used with the nautical almanac in determining the latitude and longitude by lunar observation; and keeping a complete reckoning at sea*, Fourth edition, N.Y.,, published by E. M. Blunt and Samuel A. Burtus, August 1817.

Clark, H. J., *Trajectory Versus Line-of-Sight Space Rendezvous Using Out-of-Window Visual Cues*, AMRL-TR-65-10, Aerospace Medical Research Laboratories, February 1965.

Clarke, V. C. Jr., *et al.*, *Earth-Mars Trajectories*, Jet Propulsion Laboratory, Technical Memorandum 33-100, March 1, 1967.

Duke, C. M., and Jones, M. S., *Human Performance During a Simulated Apollo Midcourse Navigation Sighting*, Massachusetts Institute of Technology, 1964, DDC No. AD 610 526.

Farber, E., *et al.*, *Manned Terminal Rendezvous Simulation Program*, Advanced Manned Systems Engineering, General Electric Company, Missile and Space Division, February 7, 1963.

Foudriat, E. C., and Wingrove, R. C., *Guidance and Control During Direct-Descent Parabolic Re-Entry*, NASA TN D-979, National Aeronautics and Space Administration, Washington, D. C., November 1961.

Havill, D. C., *An Emergency Midcourse Navigation Procedure for a Space Vehicle Returning from the Moon*, NASA-TN D-1765, 1963.

Holleman, E. C., Armstrong, N. A., and Andrews, W. H., "Utilization of the Pilot in the Launch and Injection of a Multi-Stage Orbital Vehicle", paper presented at IAS 28th Annual Meeting, New York, January 26, 1960.

Jorris, T. R., Silva, R. M., and Vallerie, E. M., *Initial Results of the Air Force Space Navigation Experiment on Gemini*, AFAL-TR-66-183, Wright Patterson Air Force Base, 1966.

Jorris, T. R., Silva, R. M., and Vallerie, E. M., *The Air Force Space Navigation Experiment on Gemini*, AFAL-TR-66-289, Wright-Patterson Air Force Base, 1966.

Lampkin, B. A. and Randle, R. J., *Investigation of a Manual Sextant Sighting Task in the Ames Midcourse N & G Simulator*, NASA TN D-2864, 1965.

Levin, E., Ward, J., *Manned Control of Orbital Rendezvous*, AD 616402, The Rand Corporation, Santa Monica, California, October 20, 1959.

Lozins, N., *Spatial Aiming of Reconnaissance Sensor*, AFAL-TR 64-324, 1964.

Miller, A. B., *Pilot Re-Entry Guidance and Control*, NASA CR-331, National Aeronautics and Space Administration, Washington, D. C. November 1965.

Miller, G. K. Jr., Fletcher, H. S., *Simulator Study of Ability of Pilots to Establish Near-Circular Lunar Orbits Using Simplified Guidance Techniques*, National Aeronautics and Space Administration, Washington, D. C. February 1965.

Moul, M. T., Schy, A. A., *A Fixed-Base Simulator Study of Piloted Entry into the Earth's Atmosphere at Parabolic Velocity*, NASA TN D-2707, National Aeronautics and Space Administration, Washington, D. C. March 1965.

Muckler, F. A., and Obermayer, R. W., *The Use of Man in Booster Guidance and Control*, NASA CR-81, National Aeronautics and Space Administration, Washington, D. C., July 1964.

Pennington, J. E., *et al.*, *Visual Aspects of a Full-Size Pilot-Controlled Simulation of the Gemini-Agena Docking*, NASA TN D-2632, National Aeronautics and Space Administration, Washington, D. C., February 1965.

Wingrove, R. C., *et al.*, *A Study of the Pilot's Ability to Control an Apollo Type Vehicle During Atmosphere Entry*, NASA TN D-2467, National Aeronautics and Space Administration, Washington, D. C., August 1964.

Appendix A

Explanation of Heliocentric Notation

(Reproduced from Jet Propulsion Laboratories TM 33-100)

Tabular listings of pertinent quantities of the heliocentric and planetocentric trajectories, differential corrections, guidance, and orbit determination parameters are given at 1-day launch date intervals and 2-day flight time intervals over the selected launch period. The launch period is selected to encompass the minimum energy transfer dates.

Each trajectory begins with a header giving launch date, flight time (in days), and arrival date. All the heliocentric transfer trajectories are calculated assuming launch into the heliocentric orbit at 0 hours of the launch date and arrival at 0 hours of the arrival date. Later, however, when the launch-planet ascent trajectories are computed, the actual launch times during the launch day for each launch azimuth are given.

Each page lists four trajectories, each of which is divided into five basic print groups: HELIOCENTRIC CONIC, PLANETOCENTRIC CONIC, DIFFEREN-TIAL CORRECTIONS, MID-COURSE EXECUTION ACCURACY, and ORBIT DETERMINATION ACCURACY. Each quantity is assigned an identifying alphabetic symbol of no more than three letters. The definitions of the symbols and quantities they represent are given below. All pertinent quantities are referenced to the mean equinox and equator, or ecliptic, of *launch* date.

A. Heliocentric Conic Group

The HELIOCENTRIC CONIC group gives the characteristics of the heliocentric transfer ellipse, such as the position and velocity vectors at launch and arrival, some orbital elements, and other quantities of engineering interest. The printout array is as follows:

HELIOCENTRIC CONIC   DISTANCE

RL LAL LOL VL   GAL AZL HCA SMA ECC INC V1

RP LAP LOP VP   GAP AZP TAL TAP RCA APO V2

RC GL GP ZAL ZAP ETS ZAE ETE ZAC ETC CLP

After the words HELIOCENTRIC CONIC, the heliocentric arc DISTANCE traveled by the spacecraft from launch to arrival is printed. The quantities are defined as follows (all angles are in deg; distances are in millions of km; speeds are in km/sec):

Column 1

RL, $R_L = |\mathbf{R}_L|$ — the heliocentric radius of the launch planet at 0 hours of the launch date.

LAL, β_L — the celestial latitude of the launch planet at 0 hours of the launch date.

LOL, λ_L — the celestial longitude of the launch planet at 0 hours of the launch date.

VL, $V_L = |\mathbf{V}_L|$ — the heliocentric speed of the probe at 0 hours of the launch date.

GAL, Γ_L — the path angle of the probe at 0 hours of the launch date, i.e., the complement of the angle between the position and velocity vectors, $\mathbf{R}_L$ and $\mathbf{V}_L$, defined by

$$\sin \Gamma_L = \frac{\mathbf{R}_L \cdot \mathbf{V}_L}{R_L V_L} \qquad -\frac{\pi}{2} \leq \Gamma_L \leq \frac{\pi}{2}$$

AZL, Σ_L — the azimuth angle of the probe at 0 hours of the launch date, i.e., the angle, measured in a plane perpendicular to the radius vector $\mathbf{R}_L$, between the projection of the ecliptic north and the projection of the velocity vector $\mathbf{V}_L$ on the plane perpendicular to $\mathbf{R}_L$, defined by

$$\cos \Sigma_L = \frac{\mathbf{V}_L \cdot \mathbf{\Psi}^1}{V_L \cos \Gamma_L} \qquad 0 \leq \Sigma_L \leq 2\pi$$

$$\sin \Sigma_L = \frac{(\mathbf{R}_L \times \mathbf{V}_L) \cdot \mathbf{\Psi}^1}{|\mathbf{R}_L \times \mathbf{V}_L|}$$

where $\mathbf{\Psi}^1 = (\mathbf{K}' - \mathbf{R}_L^1 \sin \beta_L) \sec \beta_L$, where the superscript 1 denotes a unit vector.

HCA, Ψ — the heliocentric central angle, or angle between the position vector $\mathbf{R}_L$, of the launch planet at 0 hours of the launch date and the position vector $\mathbf{R}_p$, of the target planet at 0 hours of the arrival date.

SMA, a — the semimajor axis of the heliocentric transfer ellipse.

A-1

ECC, e — the eccentricity of the heliocentric transfer ellipse.

INC, i — the inclination of the heliocentric transfer ellipse.

V1, $V_1 = |\mathbf{V}_1|$ — the heliocentric speed of the launch planet at 0 hours of the launch date.

Column 2

RP, $R_p = |\mathbf{R}_p|$ — the heliocentric radius of the target planet at 0 hours of the arrival date.

LAP, β_p — the celestial latitude of the target planet at 0 hours of the arrival date.

LOP, λ_p — the celestial longitude of the target planet at 0 hours of the arrival date.

VP, $V_p = |\mathbf{V}_p|$ — the heliocentric speed of the probe at 0 hours of the arrival date.

GAP, Γ_p — the path angle of the probe at 0 hours of the arrival date, defined the same as Γ_L except that $\mathbf{R}_p$ and $\mathbf{V}_p$ are substituted for $\mathbf{R}_L$ and $\mathbf{V}_L$.

AZP, Σ_p — the azimuth angle of the probe at 0 hours of the arrival date, defined the same as Σ_L except that $\mathbf{R}_p$ and $\mathbf{V}_p$ are substituted for $\mathbf{R}_L$ and $\mathbf{V}_L$.

TAL, v_L — the true anomaly of the probe in the heliocentric transfer ellipse at 0 hours of the launch date.

TAP, v_p — the true anomaly of the probe in the heliocentric transfer ellipse at 0 hours of the arrival date.

RCA, R_{CA} — the perihelion distance of the heliocentric transfer ellipse. This distance is printed even though the probe may not transit perihelion.

APO, R_A — the aphelion distance of the heliocentric transfer ellipse. This distance is printed even though the probe may not transit aphelion.

V2, $V_2 = |\mathbf{V}_2|$ — the heliocentric speed of the target planet at 0 hours of the arrival date.

Column 3

RC, R_c — the communication distance, or distance between the launch and target planets at 0 hours of *the arrival date.*

GL, γ_L — the angle between the launch hyperbolic-excess velocity vector $\mathbf{V}_{hL}$ and its projection on the orbital plane of the launch planet, defined by

$$\sin \gamma_L = \frac{\mathbf{W}_1 \cdot \mathbf{V}_{hL}}{V_{hL}} \qquad -\frac{\pi}{2} \le \gamma_L \le \frac{\pi}{2}$$

where $\mathbf{W}_1$ is a unit normal to the launch planet's orbital plane. This angle is useful in describing the direction in which the probe leaves the launch planet.

GP, γ_p — the angle between the incoming arrival hyperbolic-excess velocity vector $\mathbf{V}_{hp}$, and its projection on the target planet's orbital plane, defined by

$$\sin \gamma_p = \frac{\mathbf{W}_2 \cdot \mathbf{V}_{hp}}{V_{hp}} \qquad -\frac{\pi}{2} \le \gamma_p \le \frac{\pi}{2}$$

where $\mathbf{W}_2$ is a unit normal to the target planet's orbital plane. This angle is useful in determining whether the probe is approaching from above or below the target planet. If γ_p is positive, the probe approaches from below —if negative, from above.

ZAL, ζ_L — the angle between the outgoing launch asymptote (or hyperbolic-excess velocity vector) and the launch *heliocentric* radius vector $\mathbf{R}_L$ at launch time. This is the Sun–launch-planet–probe angle and is a good approximation to the launch-planet–probe–Sun angle as the probe leaves the launch planet. It is an important quantity in the design of attitude control systems which use the Sun and launch planet as optical references. The quantity ζ_L is defined as follows:

$$\cos \zeta_L = \frac{\mathbf{V}_{hL} \cdot \mathbf{R}_L^1}{V_{hL}} \qquad 0 \le \zeta_L \le \pi$$

The next six quantities, all angles, have the same general definition. They are important in the design of the near-target trajectory and are used in determining the aiming point for interplanetary flyby trajectories. Consider the target-centered geometry of Fig. A-1.
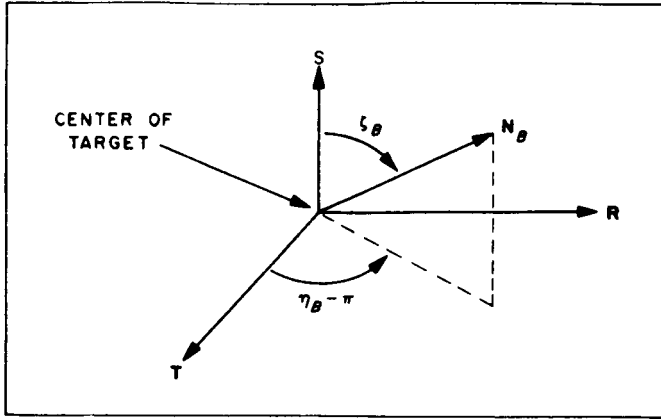
Fig. A-I. Generalized geometry for aiming point angles

In this diagram, the reference coordinate system is the same target R, S, T system defined in Section IIC. A unit vector N_B (subscript B for body) is directed from the target center to another celestial body. The angular quantity ζ_B is the angle subtended at the target center between the incoming asymptote S and the target–celestial body line N_B. Thus

$$\cos \zeta_B = S \cdot N_B = \frac{V_{hp} \cdot N_B}{V_{hp}} \qquad 0 \leq \zeta_B \leq \pi$$

since

$$S = \frac{V_{hp}}{V_{hp}}$$

The angle η_B is the supplement of the angle between the T direction and the projection of N_B on the $R - T$ plane, defined by

$$\sin \eta_B = \frac{-R \cdot N_B}{\sin \zeta_B} \qquad 0 \leq \eta_B \leq 2\pi$$

$$\cos \eta_B = \frac{-T \cdot N_B}{\sin \zeta_B}$$

These quantities are computed for three celestial bodies: the Sun (ζ_S and η_S), the Earth (ζ_E and η_E), and the star Canopus (ζ_C and η_C). Thus,

ZAP, ζ_S (or ζ_p)   the Sun–target–probe angle. Actually, this angle should be symbolized ZAS, but, for historical reasons, is not. This angle is useful in that it indicates the direction of the probe's approach to

the target. If $\zeta_S < \pi/2$, the probe approaches from the target planet's dark side. If $\zeta_S > \pi/2$, it approaches from the light side.

ETS, η_S defined as above.

ZAE, ζ_E the Earth–target–probe angle. This angle is useful in locating the Earth as the probe approaches the target.

ETE, η_E defined as above.

ZAC, ζ_C the Canopus–target–probe angle.

ETC, η_C defined as above.

CLP, σ_p the angle between the projection of the incoming asymptote S on the target planet's orbital plane and the target–Sun line at arrival time, defined by

$$\cos \sigma_p = -R_p^1 \cdot S_{pr} \qquad -\pi \leq \sigma_p \leq \pi$$

$$\sin \sigma_p = -S_{pr} \cdot (W_2 \times R_p^1)$$

where S_{pr} is the projection of S on the target's orbital plane given by

$$S_{pr} = \frac{S - W_2(S \cdot W_2)}{|S - W_2(S \cdot W_2)|}$$

Recall that W_2 is the unit normal vector to the target's orbital plane. This angle is illustrated in Fig. A-2.
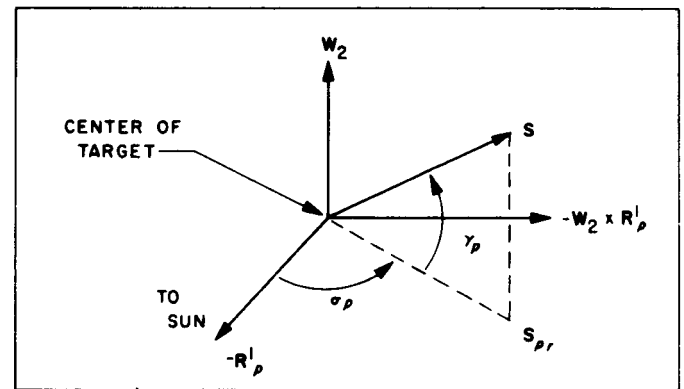

Fig. A-2. Definition of σ_p and γ_p

A-3